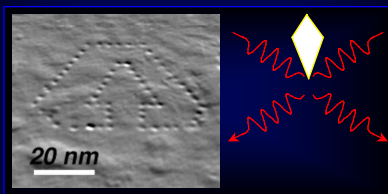


Introduction to XEDS



Nestor J. Zaluzec

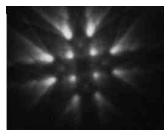
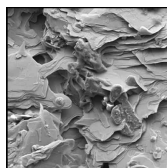
zaluzec@microscopy.com

zaluzec@aaem.amc.anl.gov

MicroCharacterization via Electron Microscopy

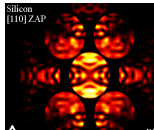
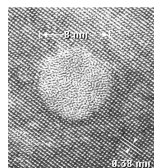
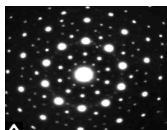
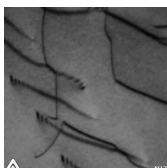
SEM

Scanning Electron Microscopy



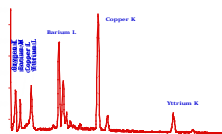
TEM - STEM - HREM

Transmission - Scanning Transmission -
High Resolution Electron Microscopy

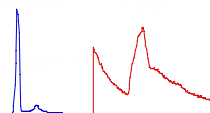


AEM

Analytical Electron
Microscopy



Intensity



Morphology, Crystallography, Elemental, Chemical, Electronic Structure

Brief Review of X-ray Generation

Instrumentation: Detector Systems

Instrumentation: EM Systems

Data Analysis and Quantification:

Additional Topics

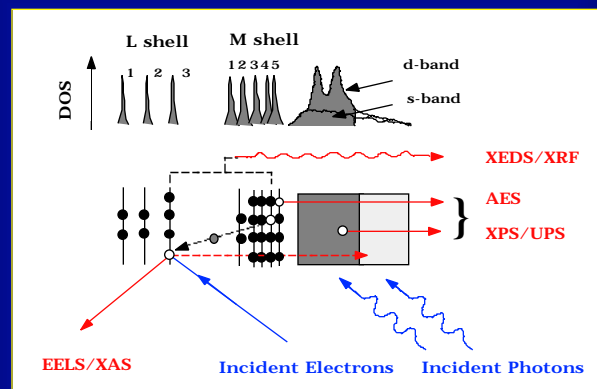
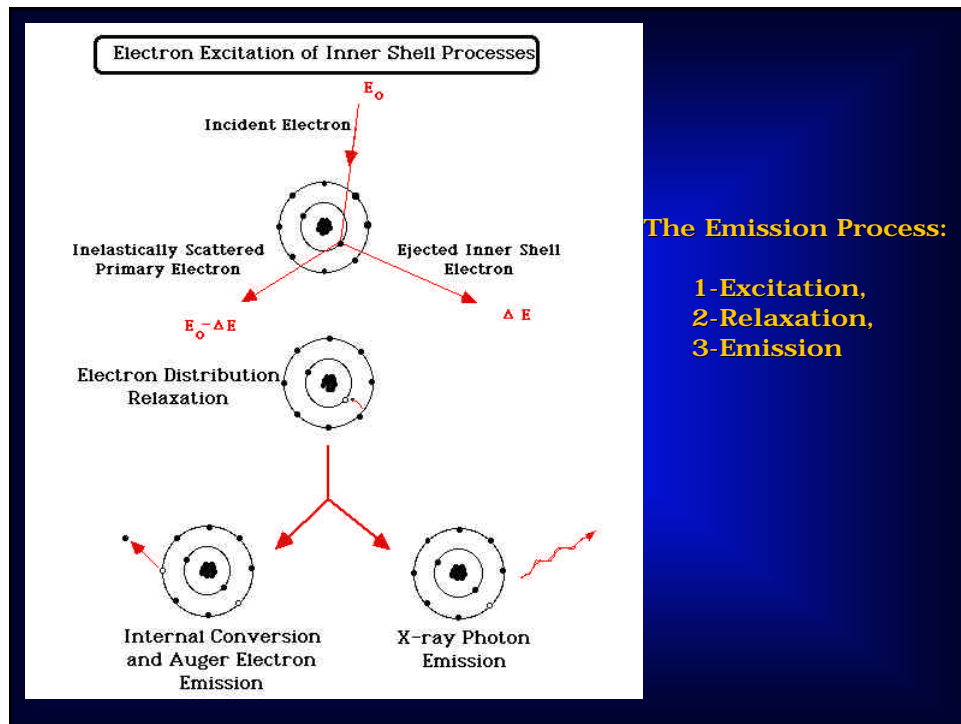
Brief Review of X-ray Generation

Electron Excitation of Inner Shell & Continuum Processes

Characteristic and Bremsstrahlung Emission

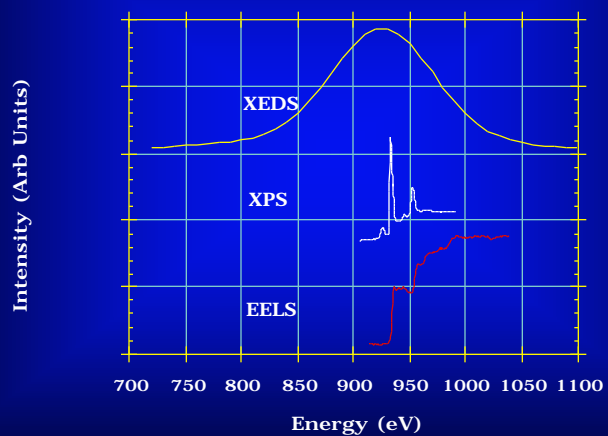
Spectral Shapes

Notation of Lines

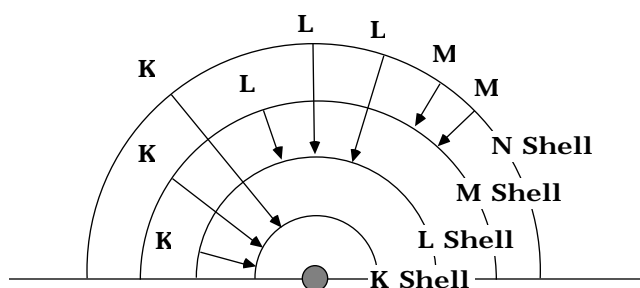


Schematic Diagram Illustrating Sources of Inelastic Scattering Signals

Experimental XEDS, XPS, and EELS data from the Copper L shell.
Note the differences in energy resolution, and spectral features.



Nomenclature for Principle X-ray Emission Lines



$$\text{Characteristic X-ray Line Energy} = E_{\text{final}} - E_{\text{initial}}$$

Recall that for each atom every shell has a unique energy level determined by the atomic configuration for that element.

$$E(K) = E_K - E_L \quad E(K) = E_K - E_M$$

X-ray line energies are unique.

$E_0 > E_x$ to "excite the x th family of lines"

Nomenclature for X-ray Lines

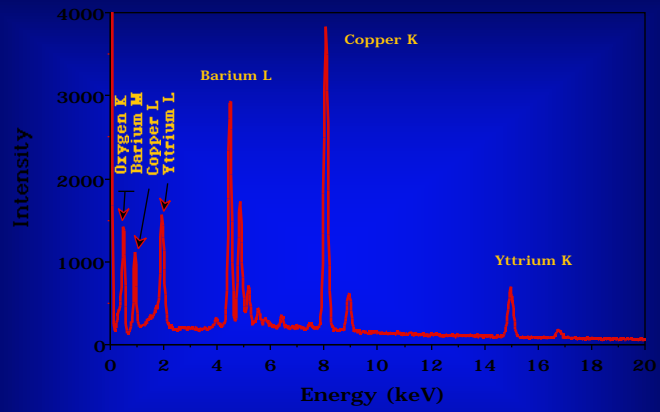
X-ray Transition Selection Rules: (Principle Quantum Numbers)

Shell	n	l	j	Rule
K	1	0	1/2	$n > 0$ $l = +1, -1$ $j = +1, 0, -1$
L	2	0, 1	1/2, 3/2	
M	3	0, 1, 2	1/2, 3/2, 5/2	
N	4	0, 1, 2, 3	1/2, 3/2, 5/2, 7/2	

Relative Intensities of Major X-ray Lines

$K_1 = 100$	$L_1 = 100$	$M_{1,2} = 100$
$K_2 = 50$	$L_2 = 50$	$M = 60$
$K_1 = 15-30$	$L_1 = 50$	
$K_2 = 1-10$	$L_2 = 20$	
$K_3 = 6-15$	$L_3 = 1-6$	
	$L_4 = 3-5$	
	$L_1 = 1-10$	
	$L_3 = 0.5-2$	
	$L = 1$	
	$L = 1-3$	

Characteristic X-Ray Spectrum Illustrating KLM lines

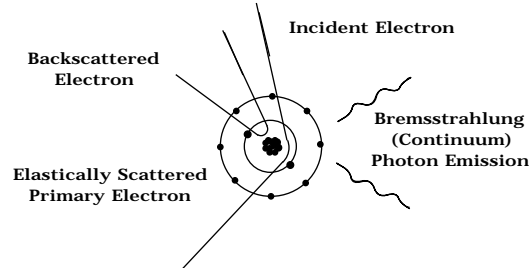


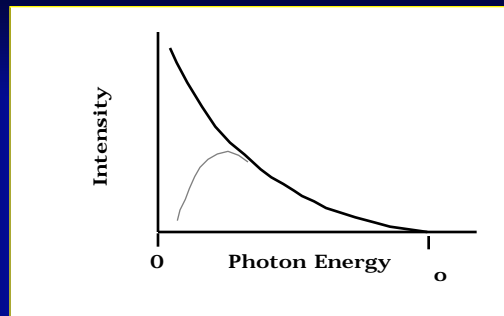
TEM Specimen: YBa₂Cu₃O_{6.9} Superconductor - 120 kV - UTW Detector

Note

As Z increases the K shell line energy increases.
If K-shell is excited then all shells are excited (Y, Ba),
but may not be detected.
Severe spectral overlap may occur for low energy lines.

Electron Excitation of Continuum Processes





Energy Range - Continuous Distribution

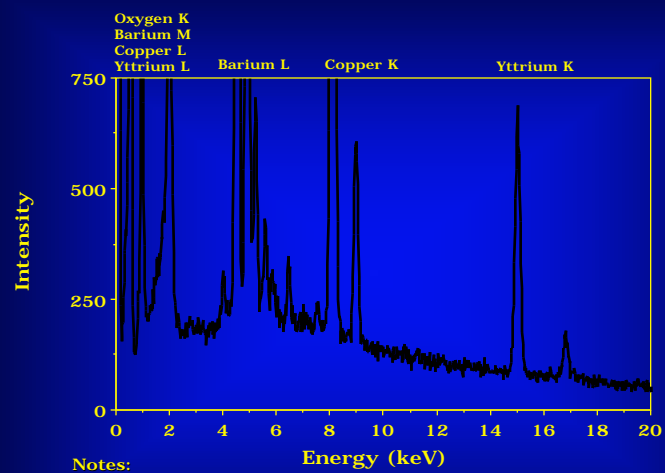
Maximum = Incident Electron Energy (Least Frequent)

Minimum = $E_{\text{plasmon}} \sim 15\text{-}30\text{eV}$ (Most Frequent)

Spectral Distribution will reflect this range, modified by detector response function

$$I \sim \frac{1}{E} Z (E_0 - E)/E$$

Electron Excitation of Continuum (Background) Intensity



Notes:

Spectral background will be influenced by:

- 1.) Specimen composition
- 2.) Detector efficiency
- 3.) TEM generated artifacts

Instrumentation: Detector Systems

Wavelength Dispersive Spectrometers (WDS)
Energy Dispersive Spectrometers (EDS)
Si(Li) Detectors
HPGe Detectors
Spectral Artifacts of the EDS System
Detector Efficiency Functions
Light Element Detectors
Superconducting (micro-calorimeters) Detectors
Multichannel Analyzers

Wavelength Dispersive Spectrometers : Diffractometer

Operates using Diffraction Principles (Bragg's Law)

Excellent Energy Resolution (~ 5 eV)
High Peak/Background Ratios (10000:1)
Good Detection Efficiency for All X-rays
High Counting Rates
Good Light Element Capabilities

Complex Mechanical Devices, Operator Intensive
Specimen Height dependant focus
Moving Components in the AEM
Limited Solid Angles (< 0.5 sr)
Serial Detection
Quantification Requires Standards

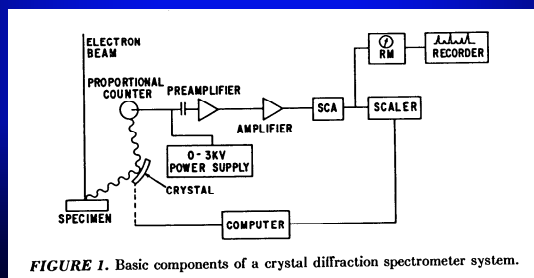
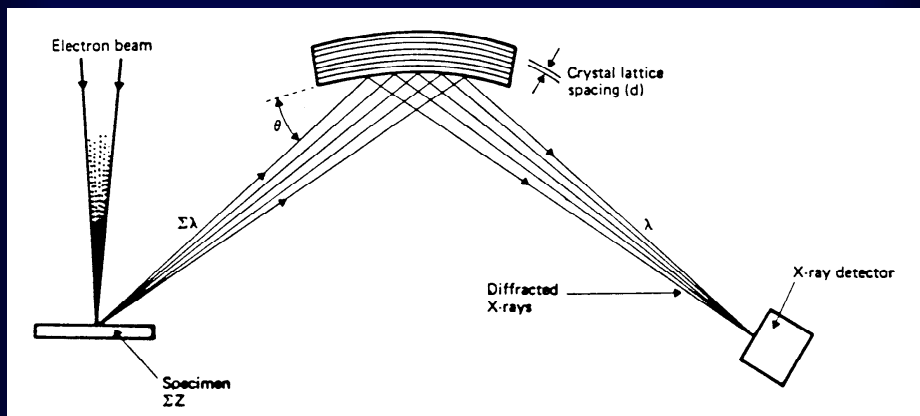


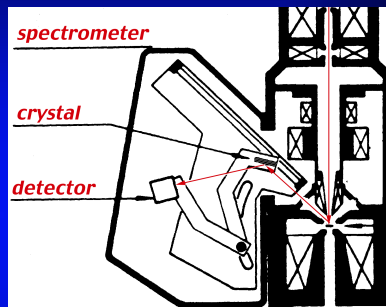
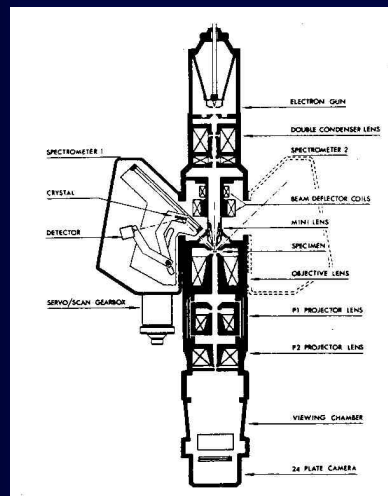
FIGURE 1. Basic components of a crystal diffraction spectrometer system.



Operation of a Crystal Spectrometer
Using Bragg's Law

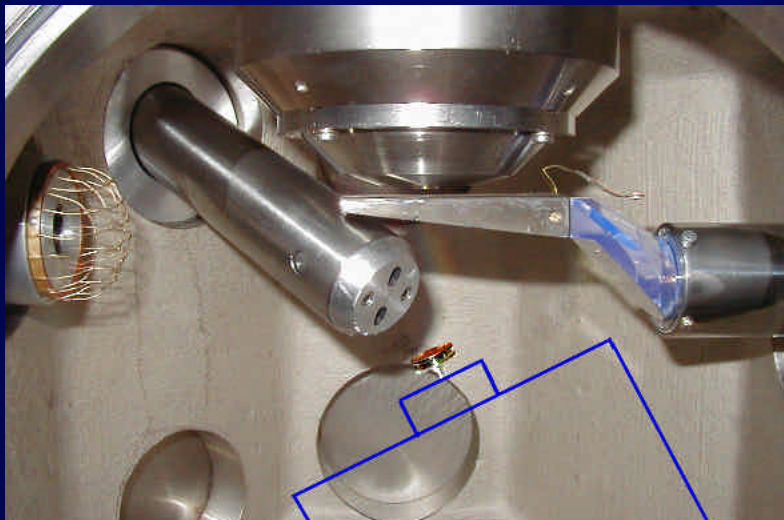
$$= 2d \sin(\theta)$$

$$= 12.398 \text{ [Å]} / \text{[keV]}$$



Installation of a Crystal Spectrometer in a
TEM - EMMA-4 System

Combined Probe / SEM Microanalysis System



Energy Dispersive Spectrometers: (Solid State Detector)

Operates on Energy Deposition Principle

Simple, Nearly Operator Independent
 Large Solid Angles (0.05-0.3)
 Virtually Specimen Position Independent
 No Moving Parts
 Parallel Detection
 Quantification by Standardless or Standards Methods

Poor Energy Resolution (~ 100)
 ** Superconducting Systems (~ 20 eV)
 Poor Peak/Background Ratios ($100:1$)
 Detection Efficiency Depends upon X-ray Energy

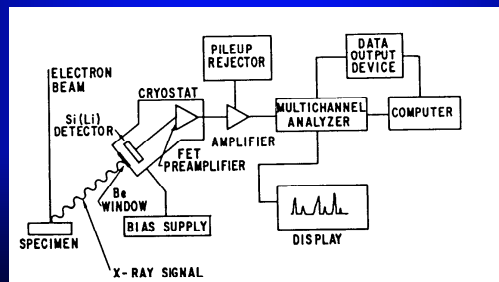
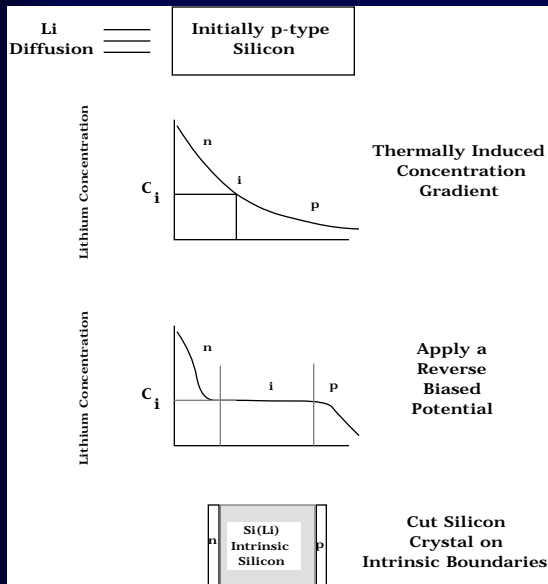


FIGURE 10. Operating schematic of a Si(Li) detector system.



• P-type Silicon high conductivity due to impurities (usually Boron); Lithium acts as a compensating dopant neutralizing the Si giving it a high resistivity

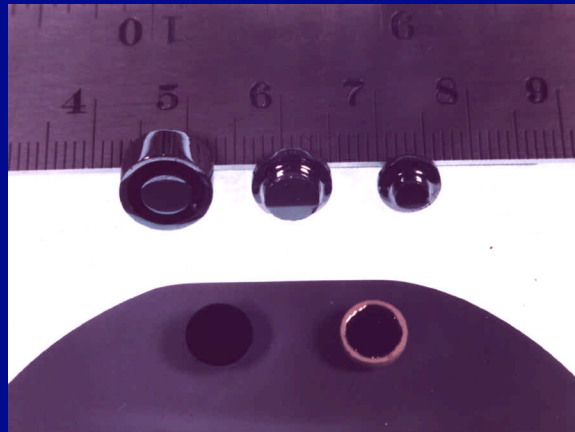
• Radiation deposits energy in the Si(Li) lattice & creates free electron-hole pairs in the crystal @ 1 electron-hole pair/3.8 eV of deposited energy @ 77K.

• Intrinsic semiconducting Si allows both electrons & holes to become mobile under application of a potential bias across the crystal

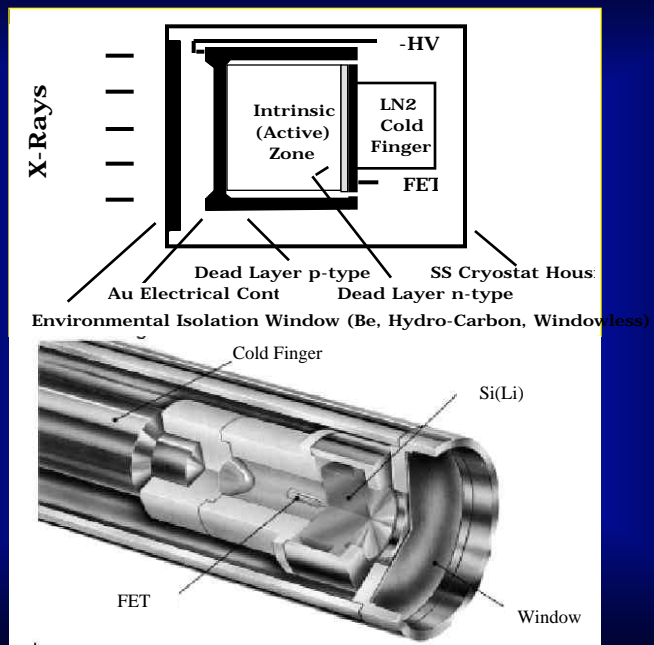
Properties of Intrinsic Silicon

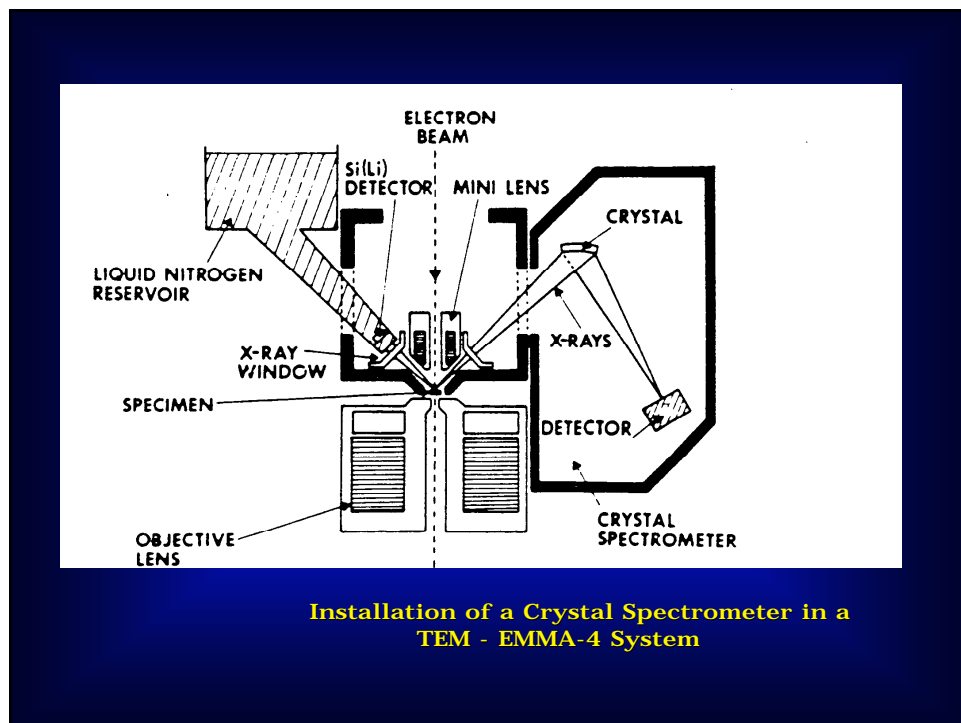
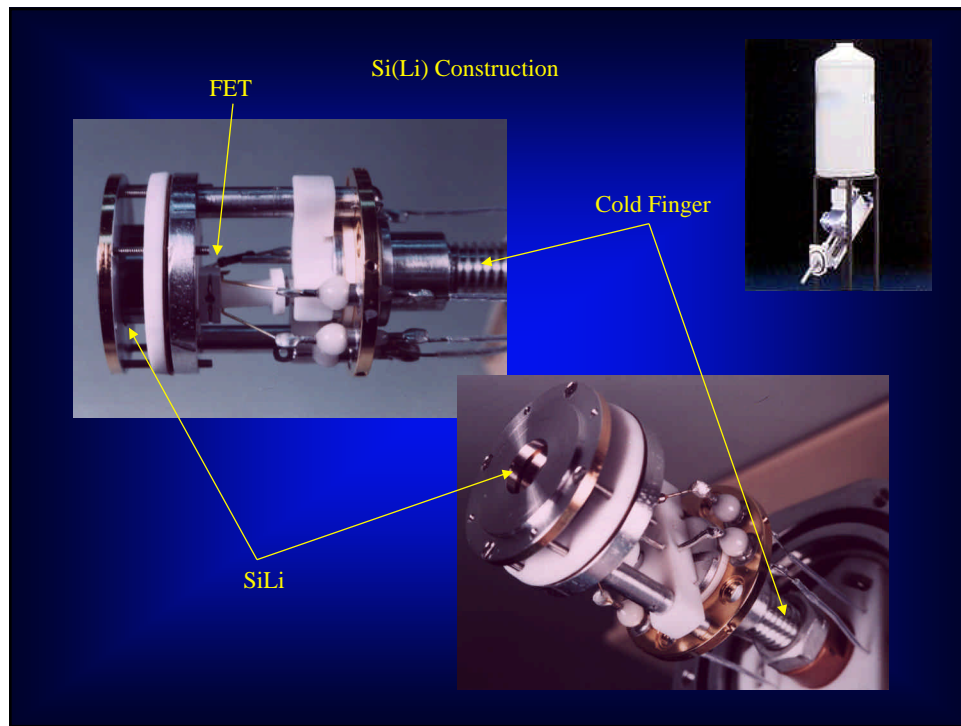
Attaching HV electrodes to the two surfaces the Si(Li) crystal will act similar to a capacitor with free charges developing on the electrical contacts. Charge developed in the crystal is $N = E / (E = \text{x-ray Energy, } = 3.8 \text{ eV/e-h pair})$ i.e. $\Rightarrow 10 \text{ kV X-ray produces } \sim 2630 \text{ electrons} = 4.2 \times 10^{-16} \text{ Coulombs}$.

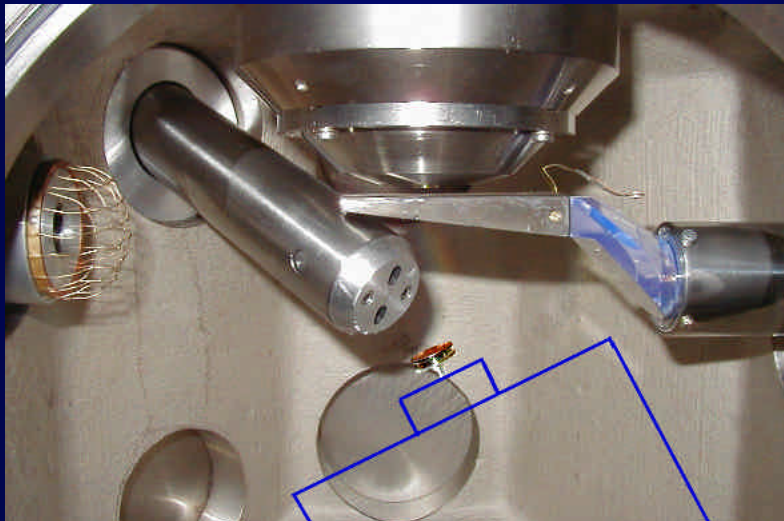
Fabrication of Si(Li) Crystals



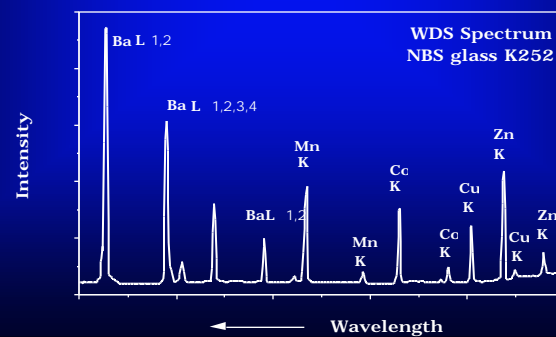
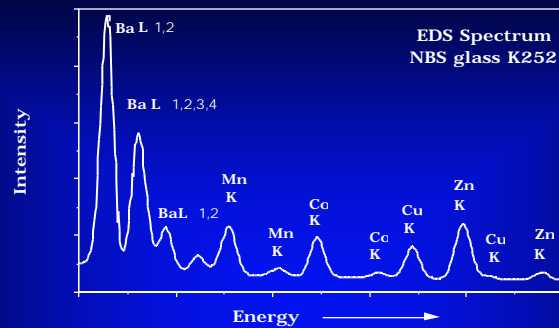
Solid State Detector Construction







Comparison of EDS and WDS Spectra

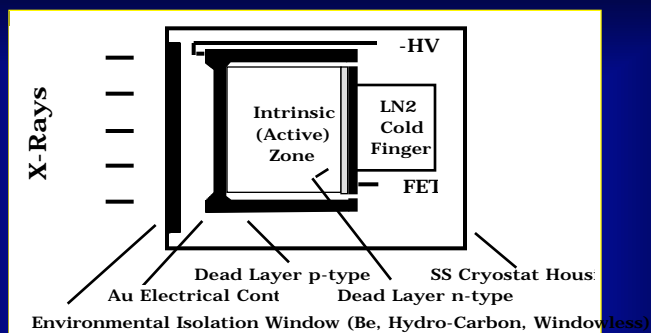


Comparison of EDS and WDS Spectrometers

Parameter	Wavelength Dispersive	Energy Dispersive
Construction	Mechanical Device moving components	Solid State no moving parts
Energy Resolution	5 eV	130 eV
Efficiency	≤ 30 %	100 % (3-15 keV)
Input Count Rate	30-50 K cps	10 K cps
Peak/Background	10000	100
Atomic Number Range	$Z \geq 4$ (Be)	$Z \geq 11$ (Na) $Z \geq 5$ (B)
Number of Elements	1 per Detector	All in Energy Range
Solid Angle	0.001-0.01 sr	0.02-0.3 sr
Collection Time	Tens of Minutes	Minutes
Beam Current	High Stability Required	Low Stability Required
Detector Stability	Good Short Term	Excellent
Spectral Artifacts	Negligible	Important
Operation	Skilled (?)	Novice

* Values depend on definition, specimen, and operating conditions

Solid State Detector Efficiency



Relative Detection Efficiency

Solid State Detectors Si(Li) or Intrinsic (High Purity) Ge
Using a simple absorption model define the relative detector efficiency by the following procedure:

$$I_0 \xrightarrow{x} I_T = I_0 \exp(-\mu x) = I_0 \exp\left(-\left[\frac{\mu}{\rho}\right] \rho x\right)$$

Relative Detection Efficiency

Solid State Detectors Si(Li) or Intrinsic (High Purity) Ge
Using a simple absorption model define the relative detector efficiency by the following procedure:

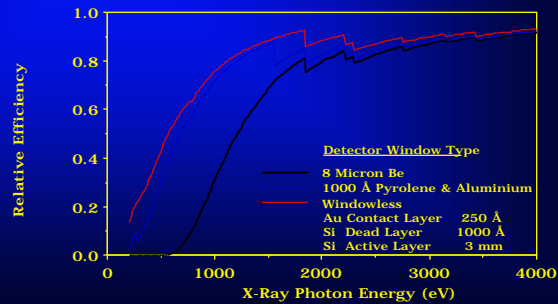
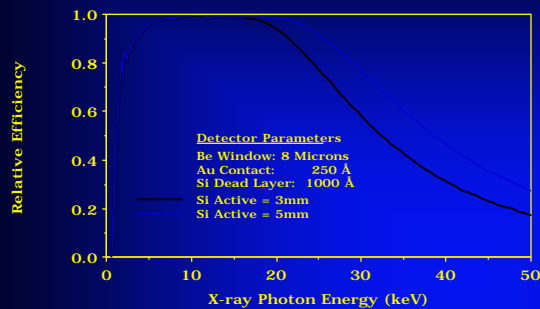
$$I_o \xrightarrow{x} I_T = I_o \exp(-\mu x) = I_o \exp\left(-\left[\sum_i \mu_i\right] x\right)$$

$$\epsilon(E) = \frac{I_A \cdot I_T}{I_o} = \exp\left(-\sum_i \left(\frac{\mu(E)}{\rho}\right)_i \cdot \rho_i \cdot t_i\right) \cdot \{1 - \exp\left(-\left(\frac{\mu(E)}{\rho}\right)_j \cdot \rho_j \cdot t_j\right)\}$$

<--Absorption--> <-- Transmission-->

$\mu(E)$ = mass absorption coefficient for Energy E; ρ = density; t = layer thickness

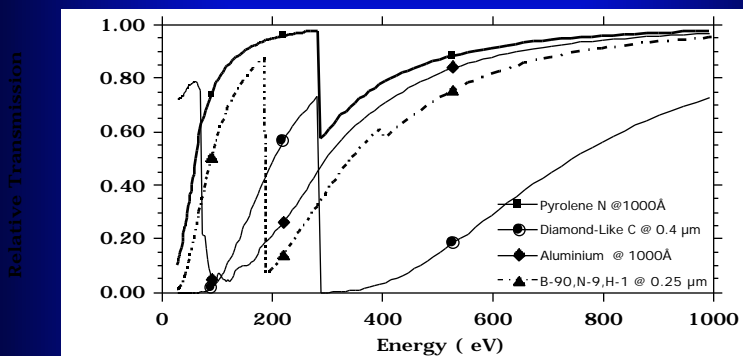
Calculated Si(Li) Detector Efficiency by Active Layer Thickness & Window Type



Relative Transmission Efficiency

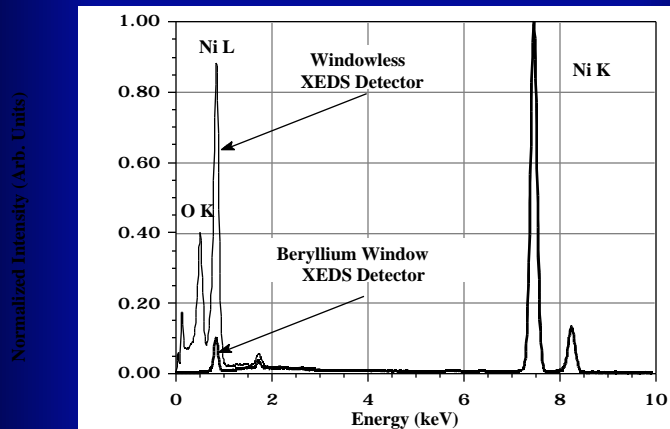
$$T(E) = \frac{I_r}{I_o} = \exp\left(-\sum_i^{\text{Window}} (\mu(E)_i \rho_i t_i)\right)$$

$\mu(E)$ = mass absorption coefficient for Energy E; ρ = density; t = layer thickness



Note the Variation in transmission characteristics by Window Type. Not all UltraThin Windows are Equivalent!!! For example Detection of Nitrogen using a Diamond window is virtually impossible.

Windowless vs Conventional Detectors Comparison of XEDS measurement of NiO using a Windowless versus Beryllium Window detector



Note the enhanced detection efficiency below 1 keV for the WL detector. Both spectra are normalized to unity at the Ni K line (7.48 keV)

Windowless vs Conventional Detectors

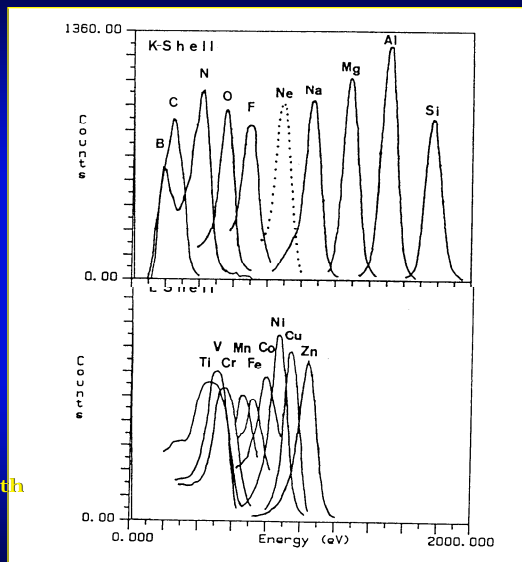
K Shell Spectra using Windowless Detector

Boron -> Silicon

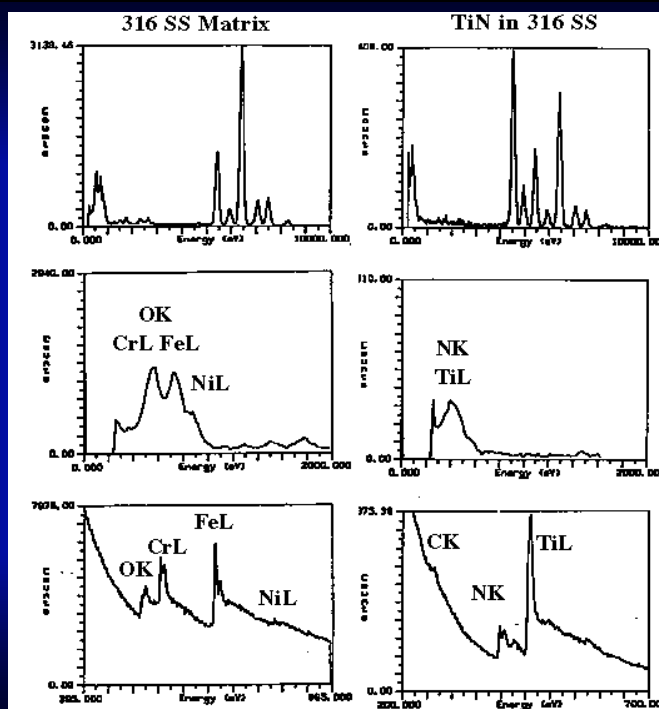
L Shell Spectra Using Windowless Detector

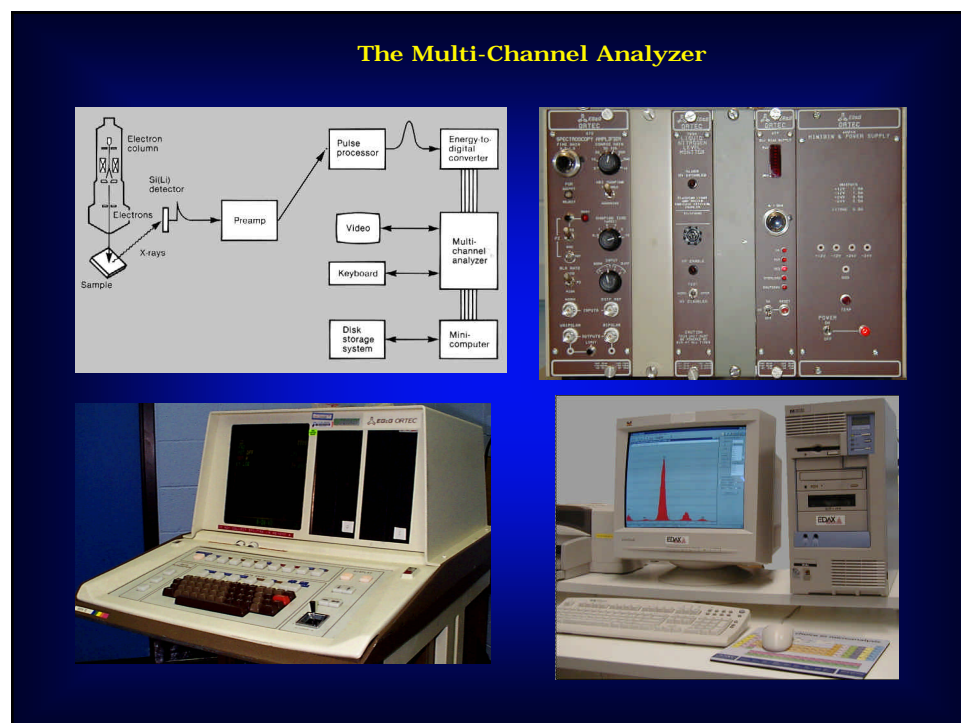
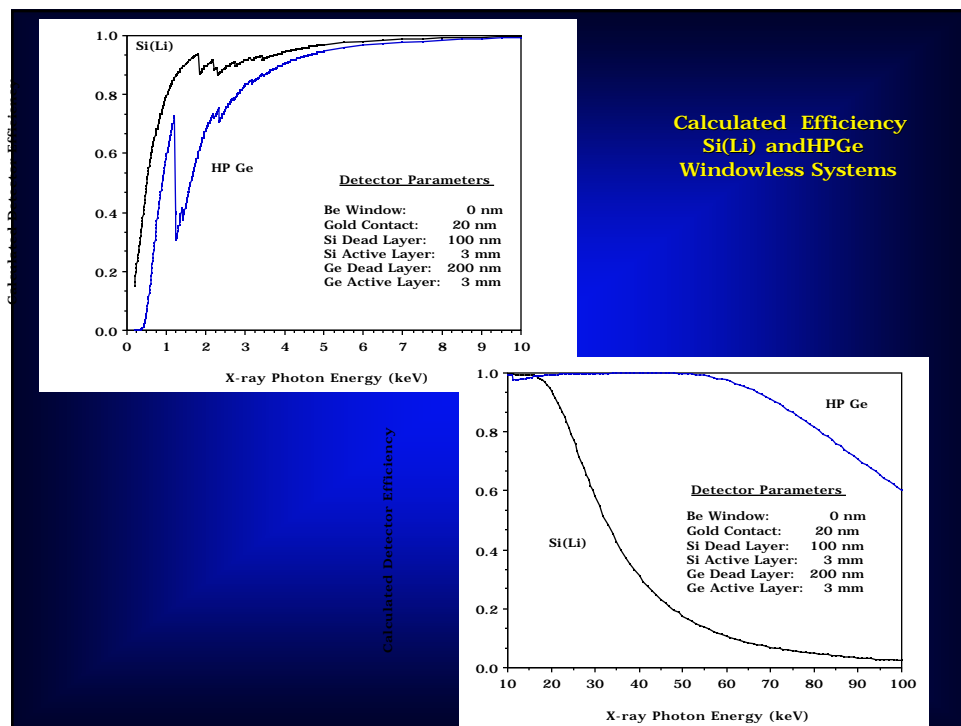
Titanium -> Zinc

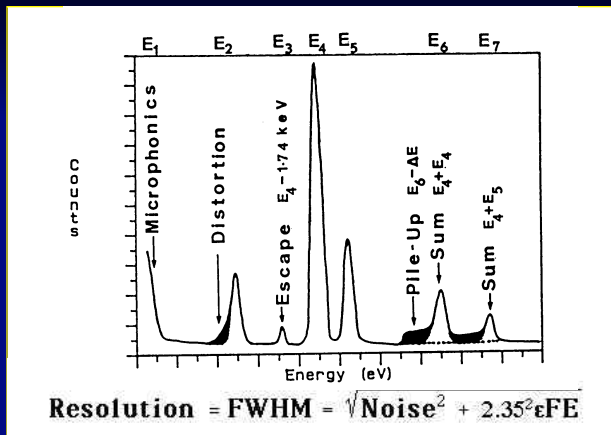
Note Potential Overlaps with K shell Lines



**Comparison
Light
Element
Spectroscopy
Resolution
XEDS vs EELS**







$$= 3.8\text{eV (InSi)} / 2.9\text{eV (InGe)}$$

F = FanoFactor ~ 0.1

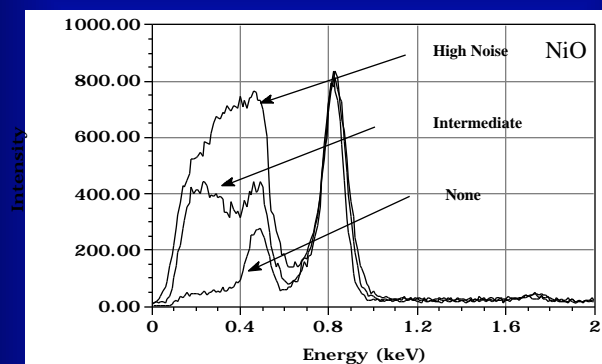
E = X-ray Energy

Noise = Electronic Noise (mainly in the FET)

Nominal FWHM Values in Modern Si(Li) Detectors:

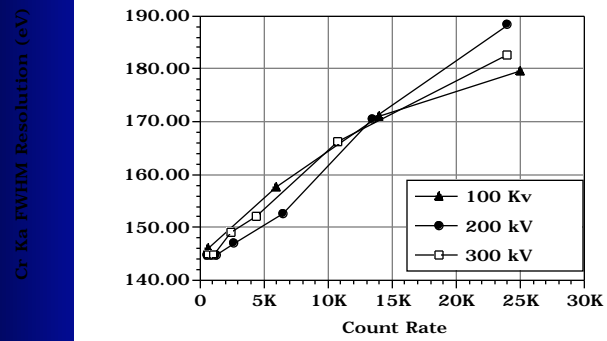
O K (0.52keV)	= 80 to 100eV
Mn K (5.9keV)	= 130 to 160eV
Mo K (17.5keV)	= 190 to 230eV

**Resolution will also vary with
Microphonic & Electronic Noise, and Counting
Rate!**



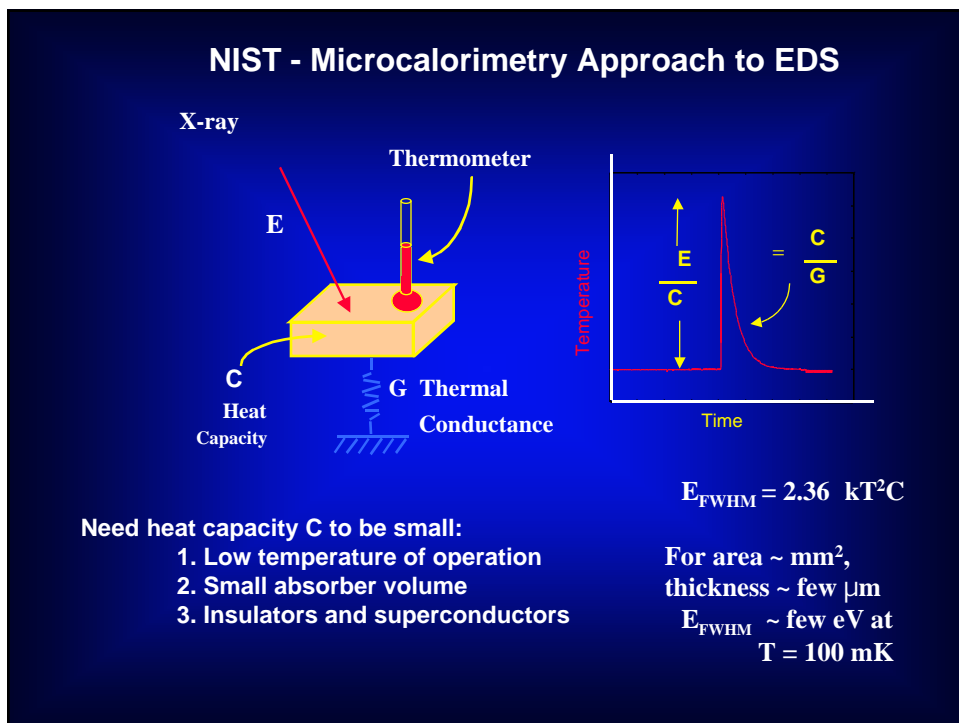
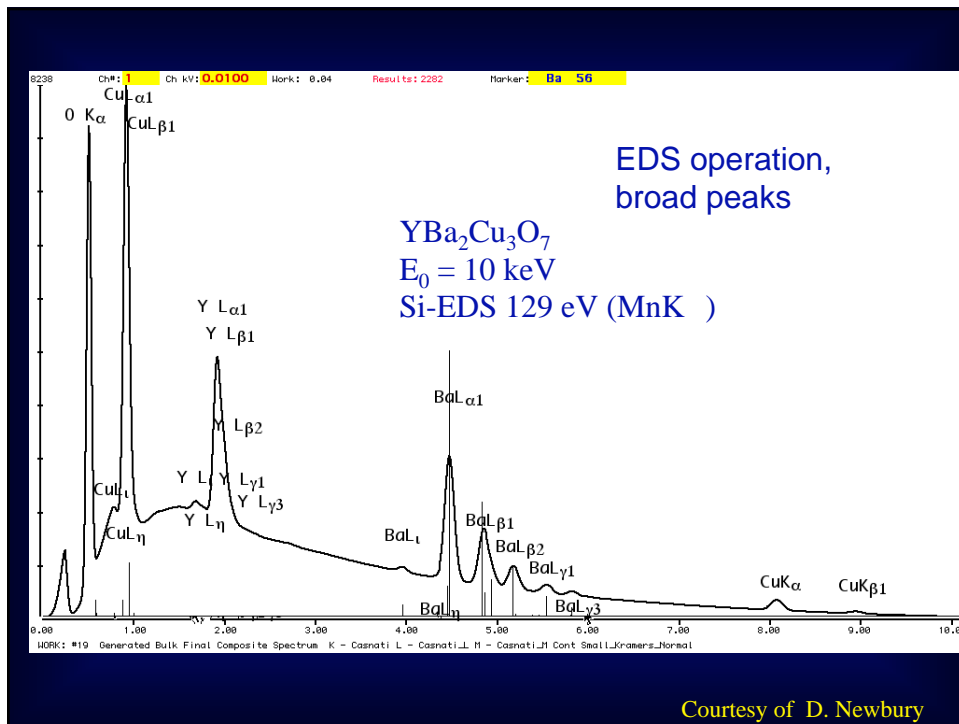
**WL & UTW detectors are particularly sensitive to low energy
noise and microphonics. Observe the changes in the spectra**

Resolution Loss with Count Rate



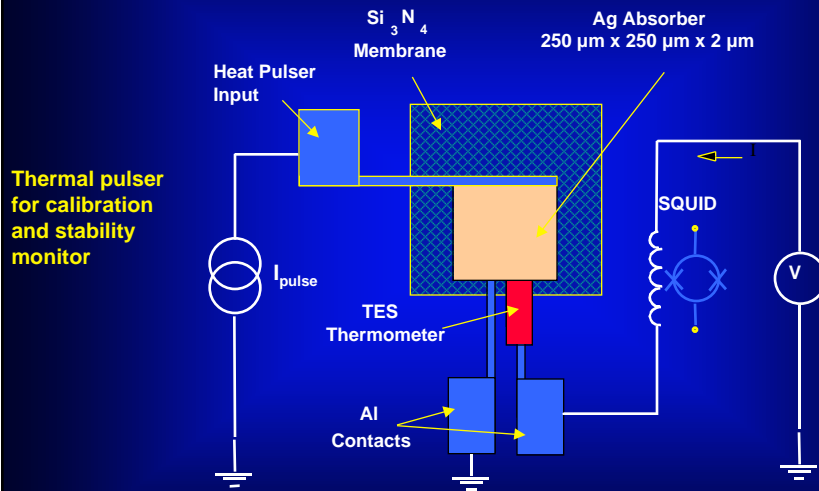
SuperConductor Detectors

Courtesy of D. Newbury

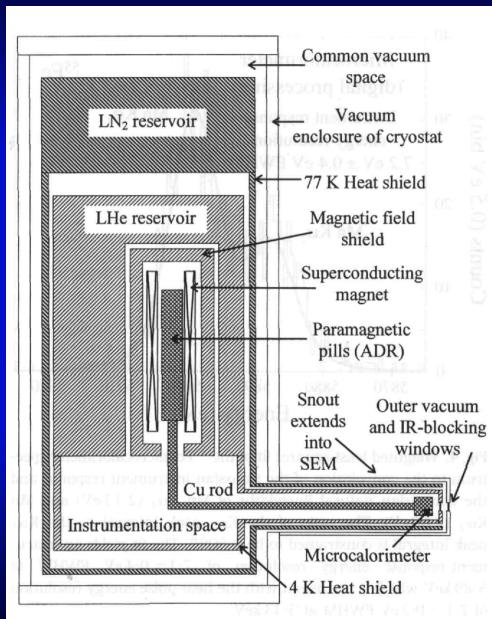


NIST Microcalorimeter X-ray Spectrometer

Cryoelectronics schematic



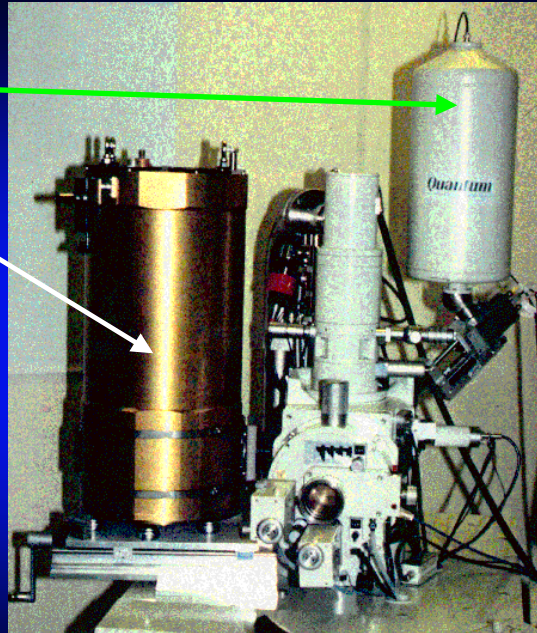
Construction of the cryostat for NIST μ cal EDS



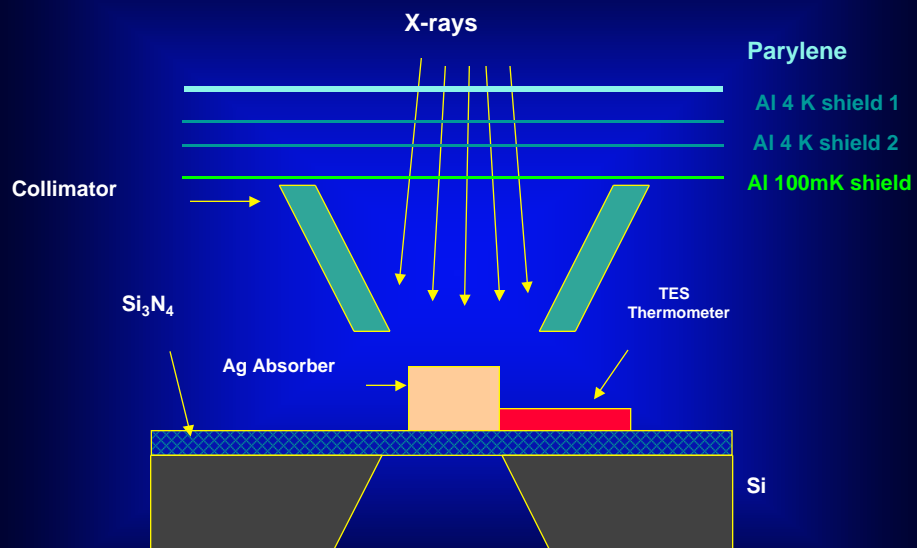
Conventional
Si(Li) EDS

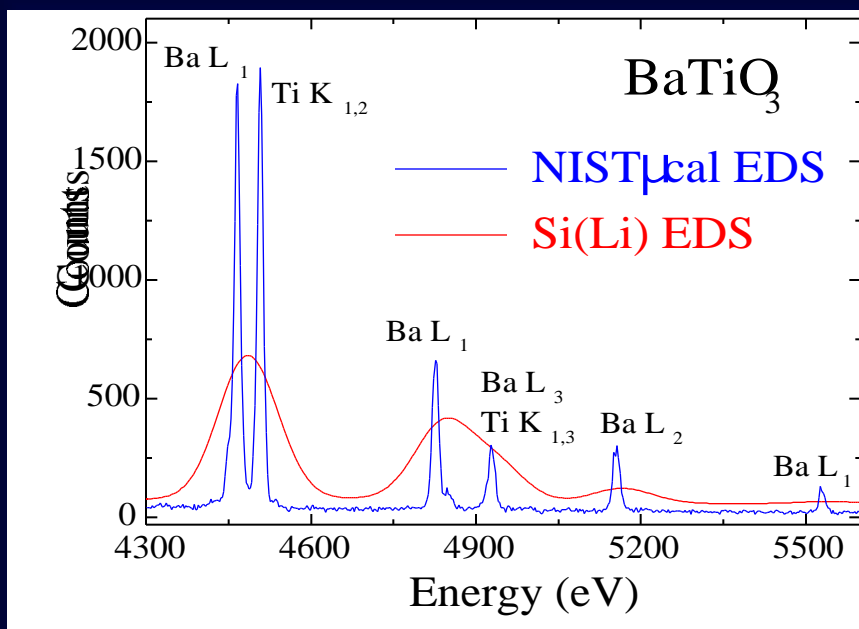
NIST
Microcalorimeter
Cryostat

1. Liquid N₂ to 77K
2. Liquid He to 4 K
3. Adiabatic demagnetization refrigerator to 100 mK



NIST Microcalorimeter X-ray Spectrometer

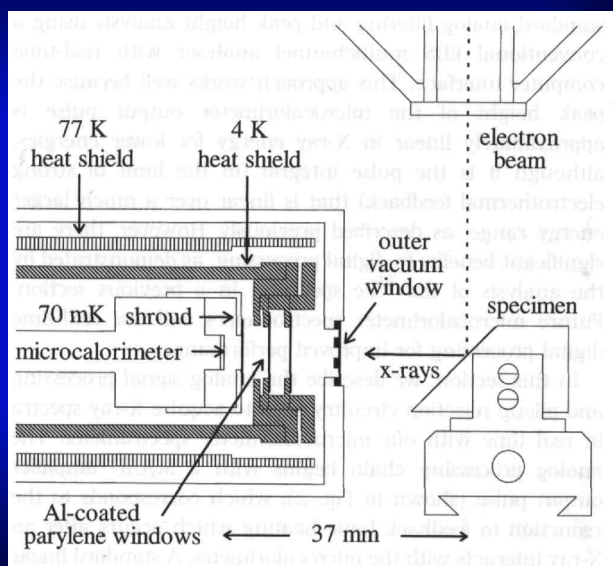




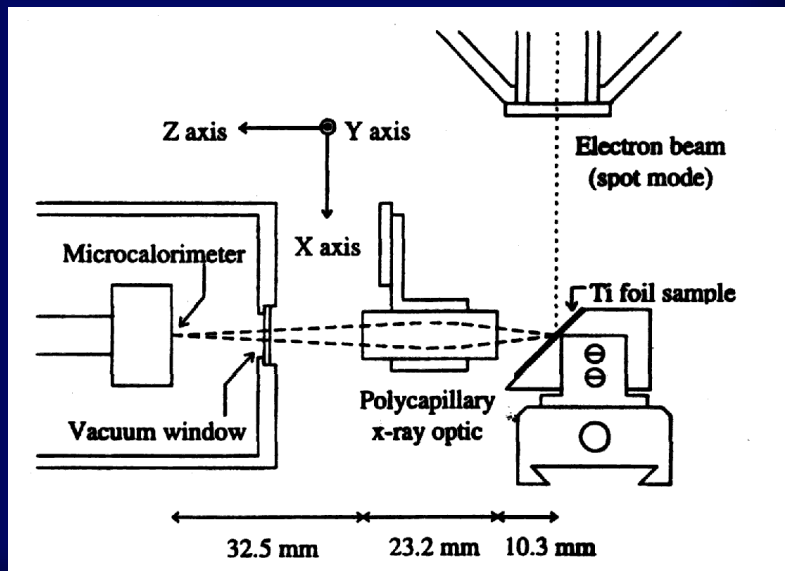
Solid angle limitations

Detector
0.5x0.5 mm
at 37 mm
= A/r^2 =
0.00018 sr

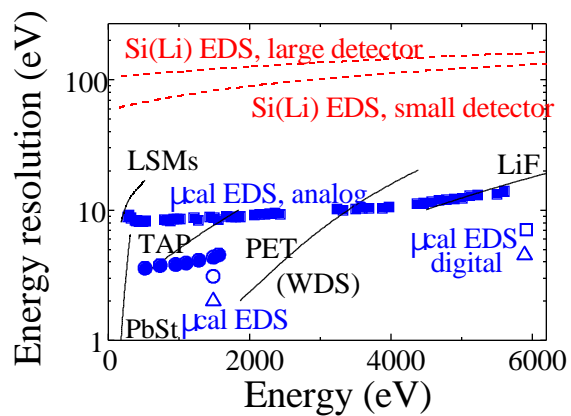
Obviously,
This is a
very small
solid angle
detector!



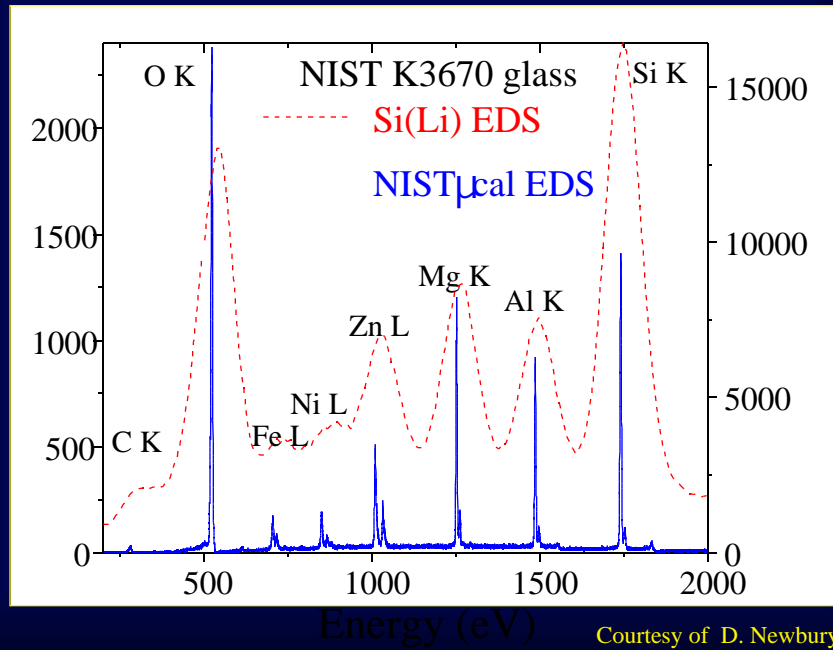
Use of Polycapillary X-ray Optic to Increase



Energy Resolution

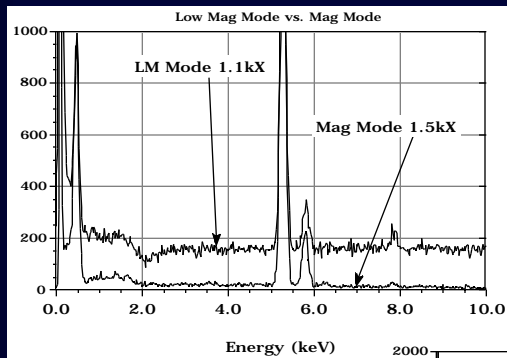


Low Photon Energy NIST Microcalorimeter



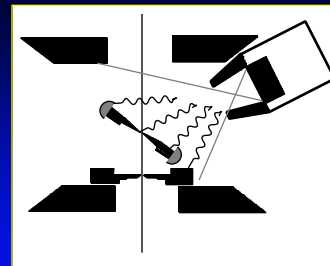
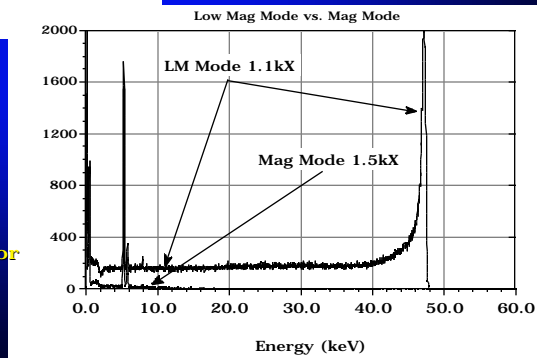
Instrumentation: SEM Systems

The SEM as a system
Spectral Artifacts in the SEM
Systems Peaks
Artifacts
Specimen Contamination & Preparation
Optimizing Experimental Conditions

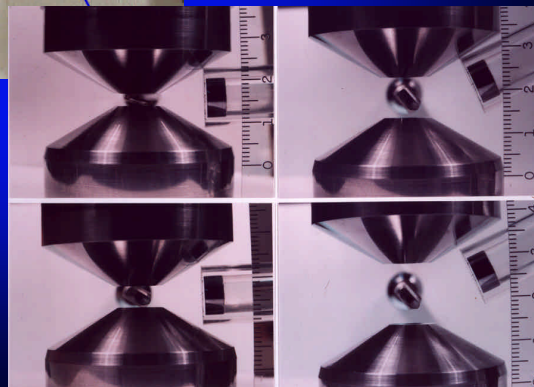


**Spectral Artifacts in the AEM:
Electrons Entering the
Detector
50 kV**

**Note the Effects of kV
Electrons Entering the Detector
on Background**



**Collimation
of the Detector
depends upon the
System Geometry**



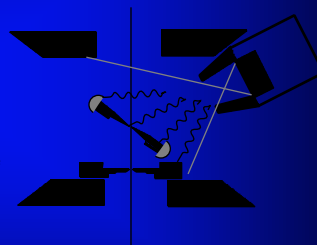


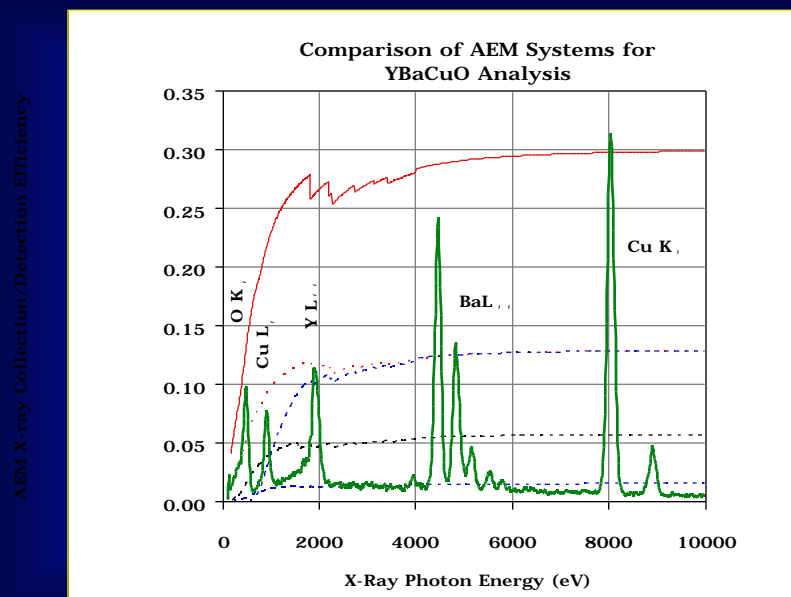
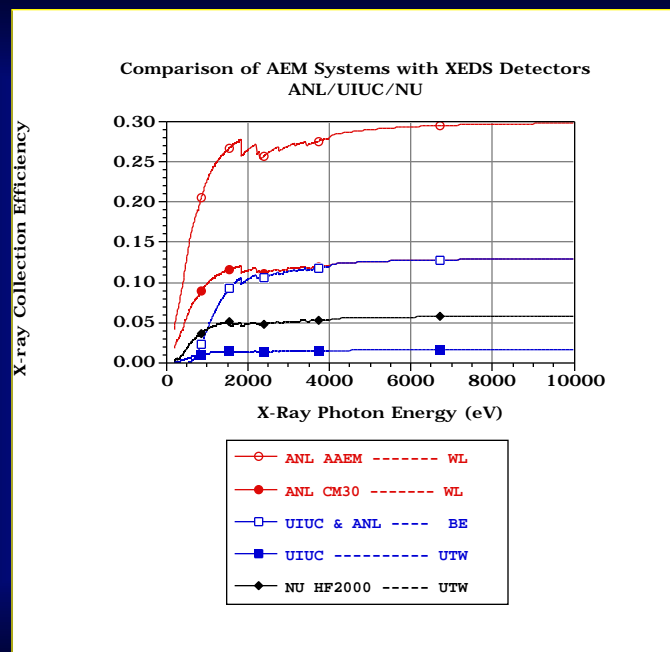
Detector/Specimen Geometry

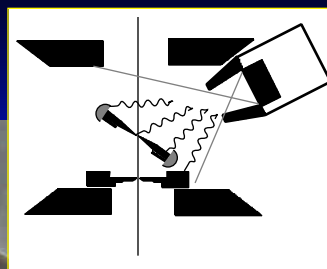
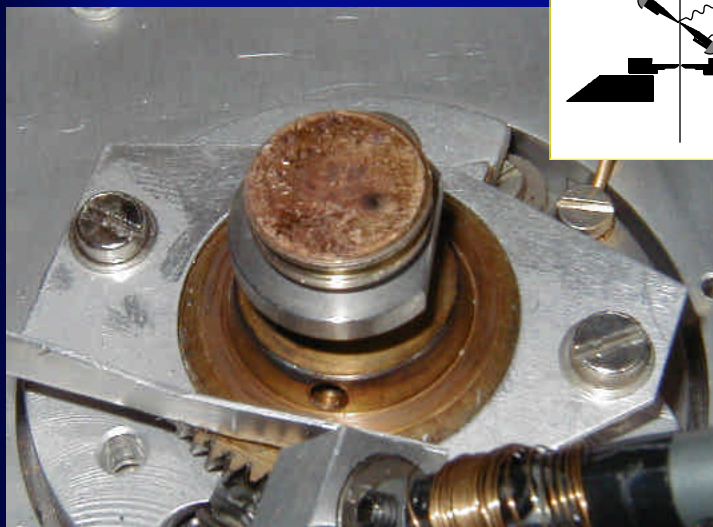
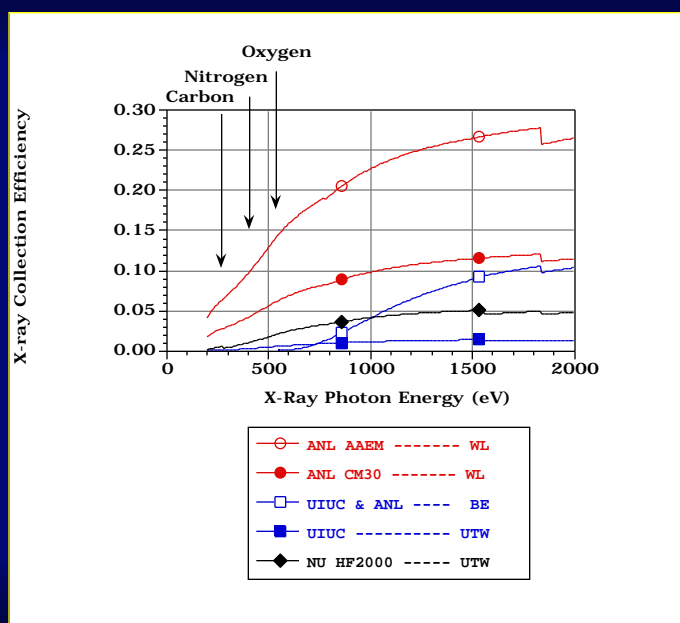
Collection Solid Angle

- $\Omega = A/R^2 = 0.3 - 0.001 \text{ sr}$
A = Detector Active Area
 = 10-30 mm²
R = Crystal to Specimen Distance
 = 10 -> ?? mm

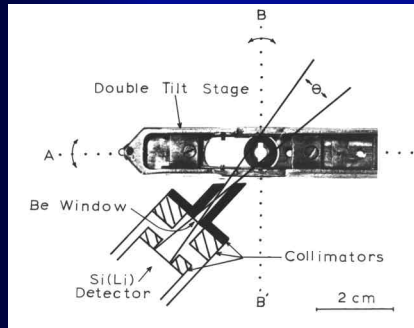
Subtending Solid Angle



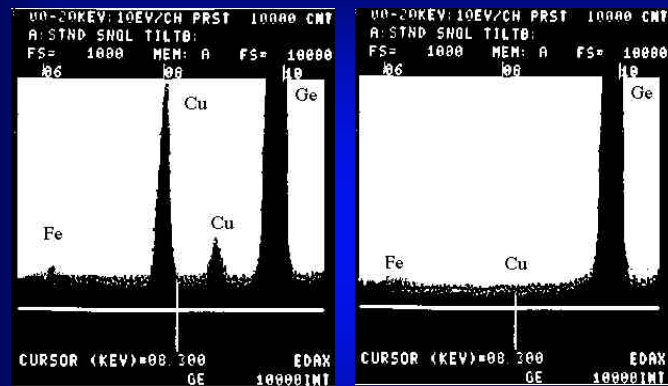




Detection of System Peaks Effects of the Collimator & Stage



Detection & Removal of System Peaks

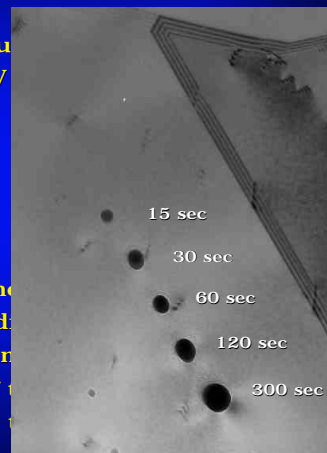


Removal of Stage System Peaks by use of Beryllium Gimbals
 Ge specimen 10,000 Ge K peak in both spectra
 Left Standard Single Tilt Cu Stage, Right GimbalDT Stage

Reactive Gas Plasma Processing Applications to Analytical Electron Microscopy

Example:

- The figure at the right shows the results of contamination formed when a 300 kV electron probe is focussed on the surface of a freshly electropolished 304 SS TEM specimen.
- The dark deposits mainly consist of hydrocarbons which diffuse across the surface of the specimen to the immediate vicinity of the electron probe. The amount of the contamination is a function of the time spent at each location. Here the time was varied from 15 - 300 seconds.

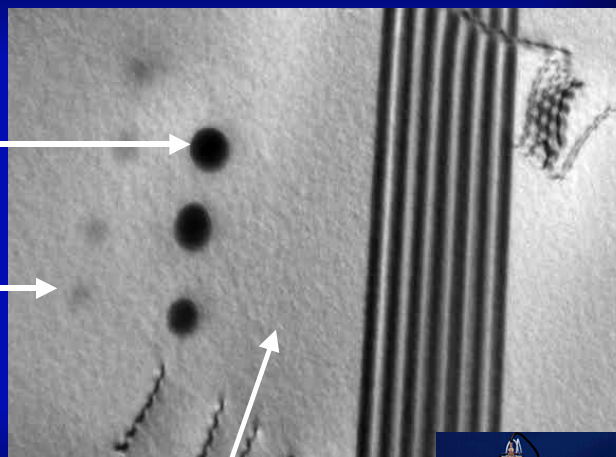


Comparison Results on Electropolished 304 SS

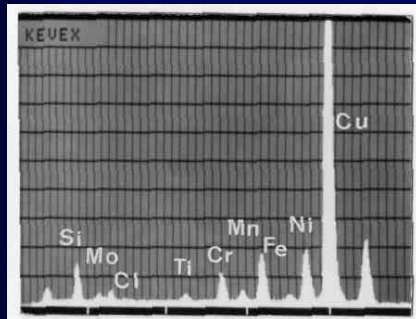
• Untreated Specimen

• After 5 minutes Argon Processing

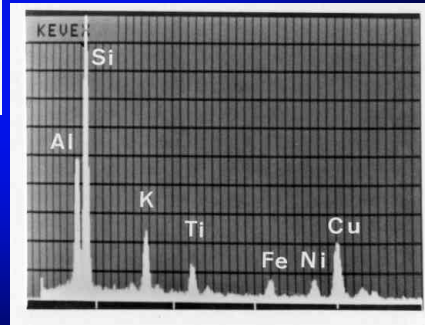
• After 5 minutes of additional Oxygen Processing



Specimen Contamination Effects



Electropolishing leaves residual Cl on surface



Ion Milling leaves redeposited Fe, Ni, Cu from SS Holder & Cu Washer

Optimizing Experimental Conditions

Choice of X-ray Line

- K- series
- L- series
- M- series

Detector/Specimen Geometry

- Elevation Angle
- Solid Angle

Detector Collimation

Choice of Accelerating Voltage

- Relative Intensity
- Peak/ Background
- Systems Peak/Uncollimated Radiation

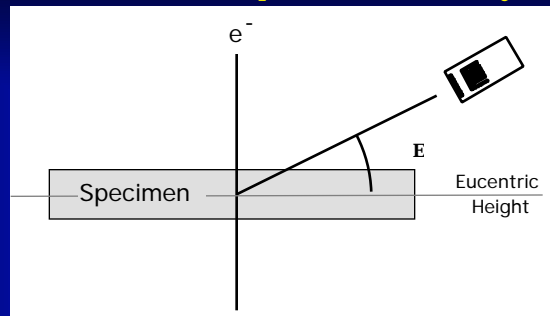
Choice of Electron Source

- Spatial Resolution
- Tungsten Hairpin
- LaB₆
- Field Emission

**Radiative Partition Function (Γ) Governs the Relative Intensities
Nominal Values (Varies slowly with Atomic Number)**

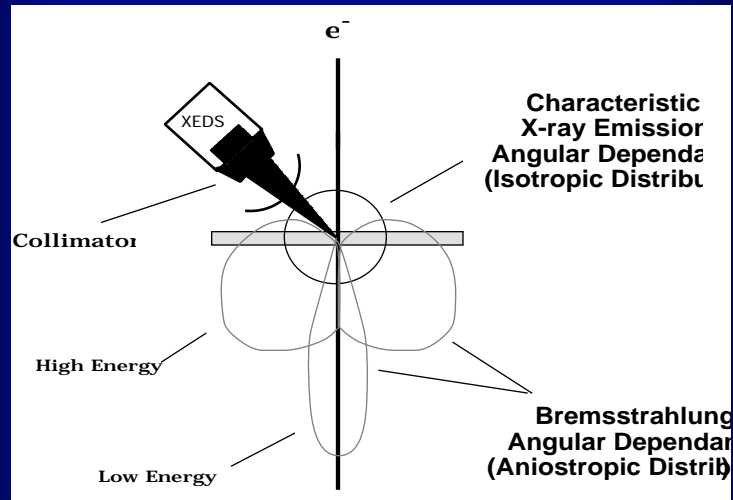
K Shell	L Shell	M Shell
$K_{\alpha 1} = 100$	$L_{\alpha 1} = 100$	$M_{\alpha 1,2} = 100$
$K_{\alpha 2} = 50$	$L_{\alpha 2} = 50$	$M_{\beta} = 60$
$K_{\beta 1} = 15-30$	$L_{\beta 1} = 50$	
$K_{\beta 2} = 1-10$	$L_{\beta 2} = 20$	
$K_{\beta 3} = 6-15$	$L_{\beta 3} = 1-6$	
	$L_{\beta 4} = 3-5$	
	$L_{\gamma 1} = 1-10$	
	$L_{\gamma 3} = 0.5-2$	
	$L_{\eta} = 1$	
	$L_i = 1-3$	

Detector/Specimen Geometry



Designation	Elevation Angle	Azimuthal Angle
	E	A
Low	0° 0°	45° 90°
Intermediate	$15-30^\circ$	90°
High	$68-72^\circ$	0°

Detector/Specimen Geometry



X-ray Production = Cross-section * electrons

$$\eta = \text{Probe current} = \frac{(\pi d_0 \alpha_0)^2 \mathcal{B}}{4}$$

$$\mathcal{B} = \text{Brightness} = \left(\frac{I_c}{\pi k T} \right) e V_r$$

$$V_r = \text{Relativistic Voltage} = V_0 \left(1 + \frac{e V_0}{2 m_0 c^2} \right)$$

$$V_0 (1 + 9.785 \times 10^{-7} V_0)$$

Non-Relativistic Cross-section Model

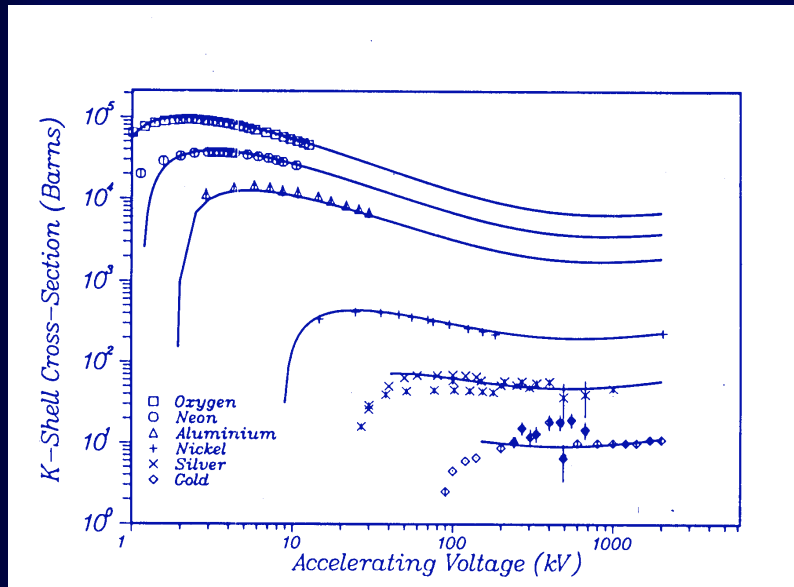
$$Q_K = \frac{a_K * b_K * \left\{ \ln \left(c_K * \frac{E_0}{E_c} \right) \right\}}{E_0 E_c}$$

Relativistic Cross-section Model

$$Q_K = \frac{a_K * b_K * \left\{ \ln \left(c_K * \frac{T_0}{E_c} \right) - \ln(1 - \beta^2) - \beta^2 \right\}}{T_0 * E_c}$$

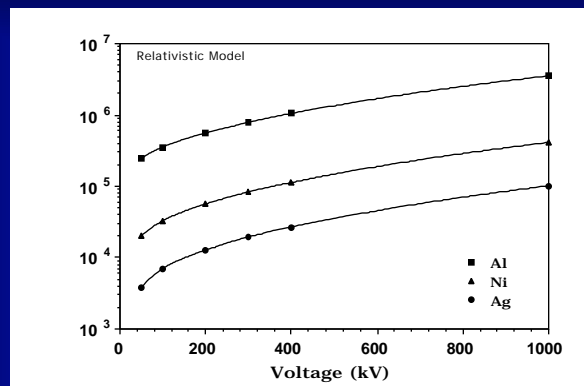
$$T_0 = \frac{1}{2} m_0 c^2 \beta^2, \text{ where } \beta = v/c$$

Maximizing
The Signal



Effects on Intensity with Accelerating Voltage for constant Probe size parameters

Relative Number of K-shell Ionizations



$$I = Q *$$

For identical probe diameters one has higher x-ray production at higher voltage due to the increase in beam current.
Alternatively, one can achieve the same statistical intensity for smaller probes at higher

Minimum Detectable Mass

$$\text{MDM} \sim \frac{k}{P_x I_o \tau} = \frac{k^*}{P_x J_o d_o^2 \tau} -$$

Minimum Mass Fraction

$$\text{MMF} \sim \frac{k}{\sqrt{[P_x (\frac{P}{B})_x] I_o \tau}} = \frac{k^*}{\sqrt{[P_x (\frac{P}{B})_x] J_o d_o^2 \tau}}$$

$k, k^* = \text{Constants}$

$P_x = \text{Characteristic Signal}$
from element X

$(P/B)_x = \text{Peak to Background ratio for element X}$

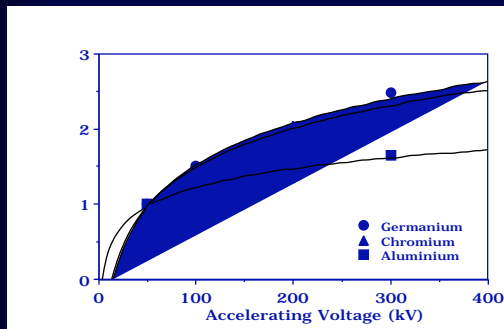
$I_o = \text{Incident electron flux}$

$J_o = \text{Incident electron current density}$

$d_o = \text{Probe diameter}$

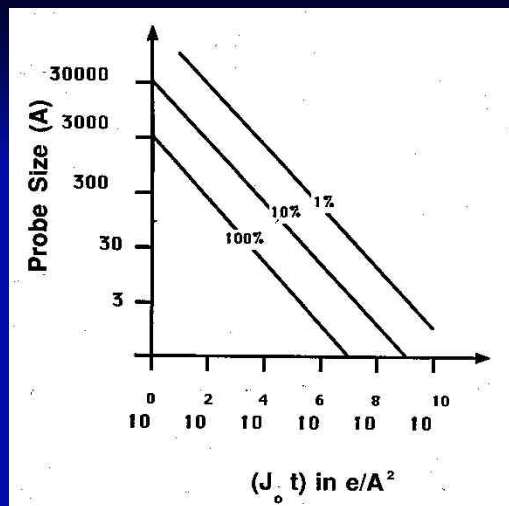
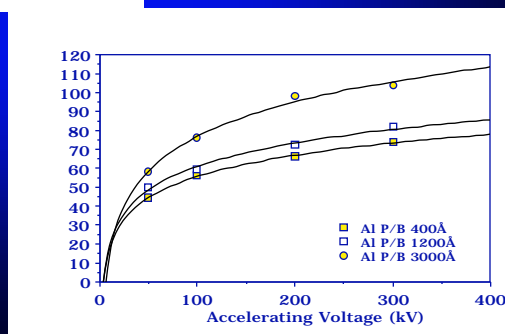
$\tau = \text{Analysis time}$

Normalized Peak/Background Ratio



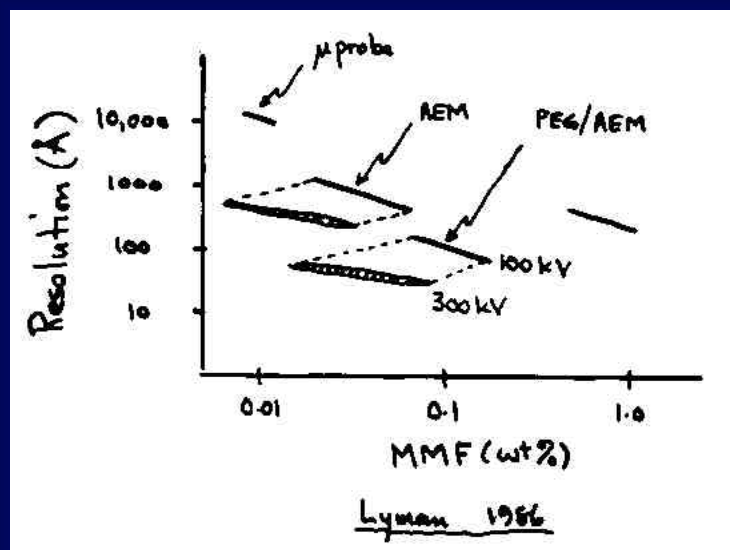
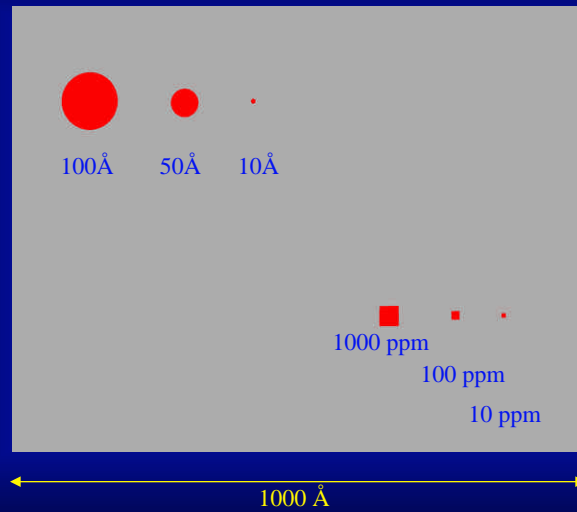
Experimental Peak/Background Variation with Voltage

Aluminium Peak/Background Ratio

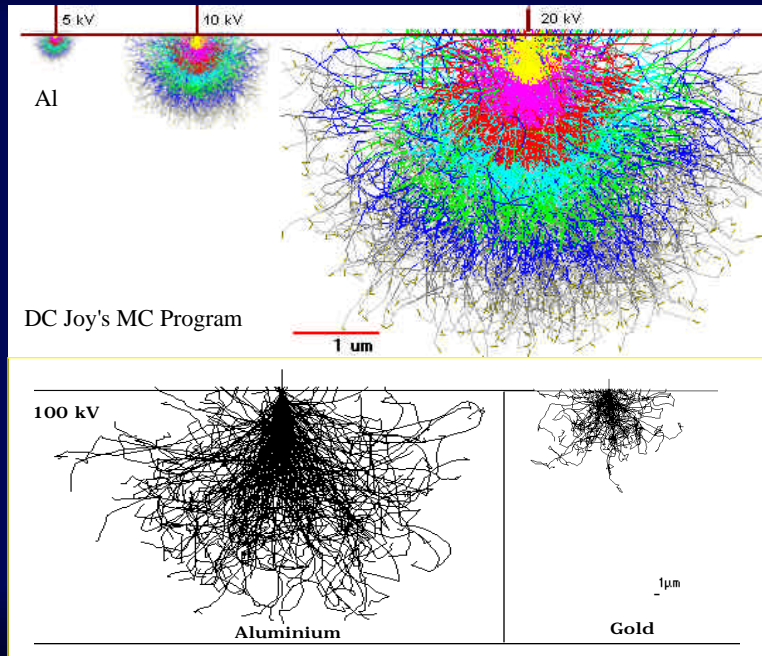


$$d_o = \frac{k}{MMF} \left[\frac{1}{P_x (P/B)_x J_0 t} \right]^{1/2}$$

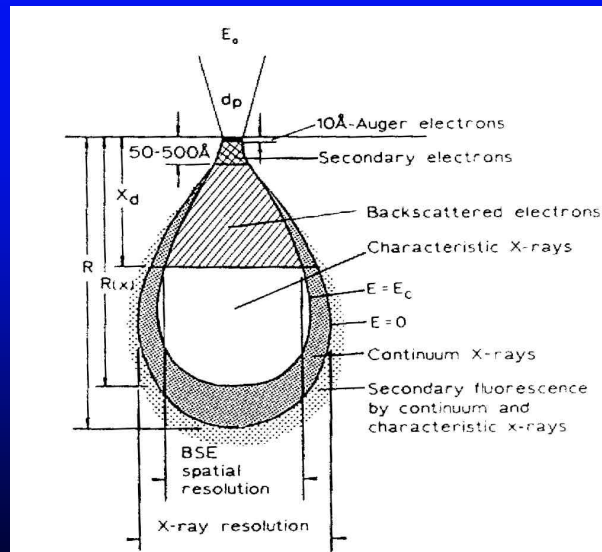
Minimum Detectable Mass

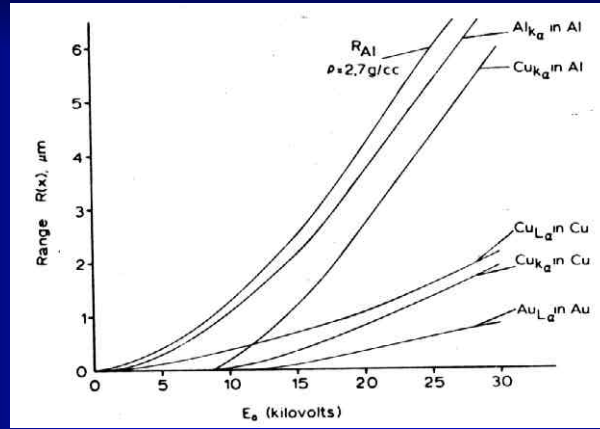


Spatial Resolution /Beam Spreading Monte Carlo Calculations



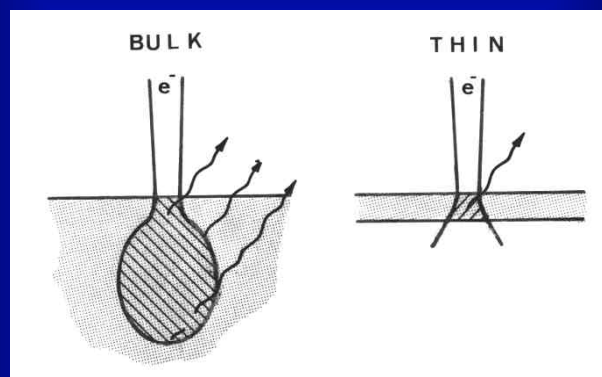
Depth Distribution

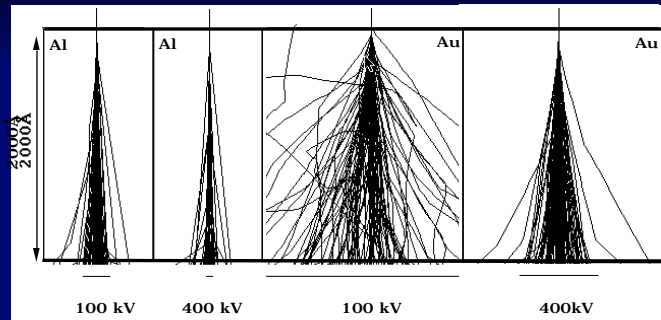




Goldstein

$$R [\mu\text{m}] = 0.231 (E_0[\text{kV}]^{1.5} - E_c[\text{kV}]^{1.5}) / [\rho[\text{g}/\text{cm}^3]] \quad (\text{Reed})$$





Monte Carlo Calculations of(Newbury & Myklebust-1979)

Element	Z	Thickness			
		10nm	50nm	100nm	500nm
Carbon	6	0.22	1.9	4.1	33.0
Aluminium	13	0.41	3.0	7.6	66.4
Copper	29	0.78	5.8	17.5	244.0
Gold	79	1.71	15.0	52.2	1725.0

Analytic Formulation (Elastic Scattering - Goldstein etal 1977)

$$B = 625 \frac{Z}{E_0} \sqrt{\frac{\rho}{A}} t^{3/2}$$

B = Beam Broadening [cm]

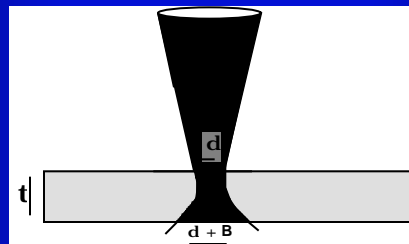
Z = Atomic Number

E₀ = Accelerating Voltage [kV]

ρ = Density [gms/cm³]

A = Atomic Weight

t = Thickness [cm]

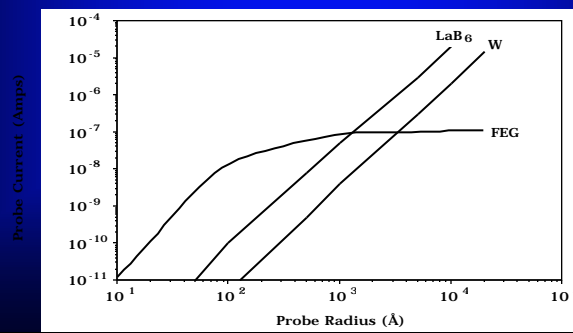


Element	Z	10nm	50nm	100nm	500nm
Carbon	6	0.16	1.8	5.13	57.4
Aluminium	13	0.26	1.9	8.12	90.9
Copper	29	0.68	7.6	21.4	*
Gold	79	15.5	17.3	*	*

*model invalid at higher kV and/or high scattering angles

Comparison of Electron Sources

Type		Brightness $/Vo$ $A/cm^2/mr/eV$	Source Size (μm)	Energy Spread (eV)	Noise	Stability	Cohereny	Vacuum (Torr)
Thermionic	Hairpin	1	50	2-3	Low	Good	Low	$<10^{-4}$
	Pointed	5	10			Fair	Moderate	$<10^{-5}$
LaB ₆	Poly Crystal	10-30	10	~1	Low	Good	Moderate	$<10^{-6}$
	Single Crystal	20-50	5					
Field Emission	Thermal Assist	100-500	$<100\text{\AA}$	~.5	Fair	Moderate	High	$<10^{-8}$
	Cold	100-1000		$<.25$		Fair		$<10^{-10}$

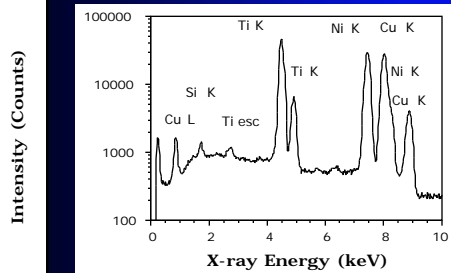


Data Analysis and Quantification:

Spectral Processing
Quantification Methods

Spectral Processing : XEDS

Spectrum = Characteristic Peaks + Background



Data Reduction

Simple: Linear Background Fit & Integration

Curve Fitting: Non-Linear Background & Profile Matching

Frequency (Digital) Filtering: Background Suppression & Reference Spectra Fitting

Deconvolution Fourier Method for Resolution Enhancement

Background Modeling

Simple - Linear and/or Polynomial Interpolation

Modeling - Parametric Fits of Analytic Expressions

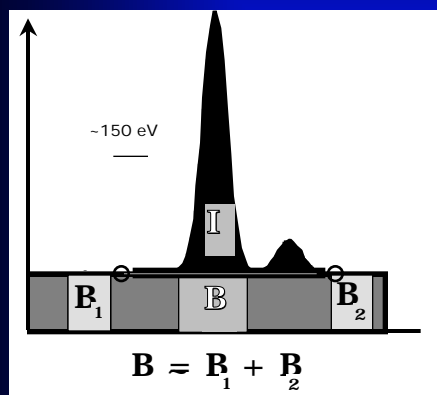
Phenomenological Expressions

Modified Bethe Heitler Model

Digital Filtering - Mathematical Suppression

Spectral Processing : XEDS

Simple Data Reduction



Note: Must use peak integrals (I) and not peak amplitudes (A)

Recall that for Gaussian Peak

$$I = \int_{-\infty}^{+\infty} A \exp\left(-\frac{x^2}{2\sigma^2}\right) dx = \sqrt{2\pi} \sigma A$$

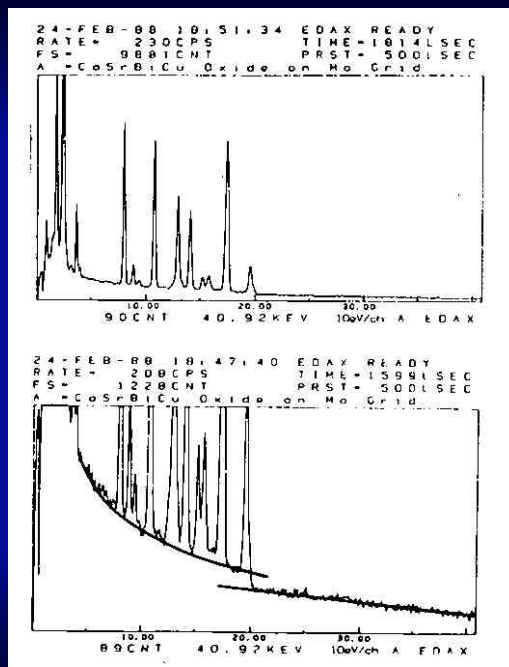
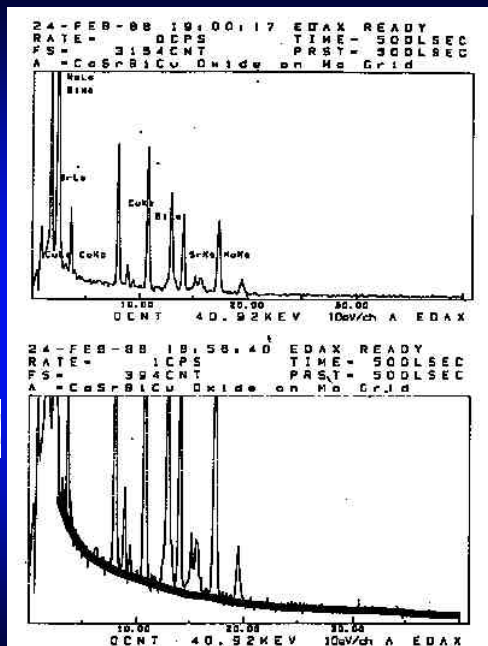
Hence for the ratio of Intensities

$$\frac{I_1}{I_2} = \frac{\sigma_1^2 A_1}{\sigma_2^2 A_2} \neq \frac{A_1}{A_2}$$

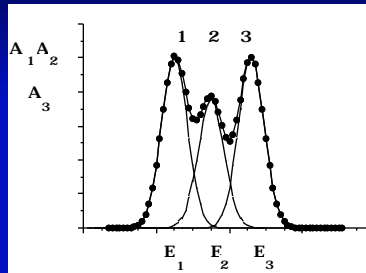
**Spectral Processing :
XEDS**

**Background Modeling :
Power Law/Parametric
Fits**

$$\text{Bgnd} = * \left(A \left(\frac{E-E_0}{E} \right)^2 + B \left(\frac{E-E_0}{E} \right) + C \right)$$



Spectral Processing : XEDS Curve Fitting : Linear Modeling



Let

$$G_{ij} = \exp \left(\frac{-(E_j - E_i)^2}{2\sigma_{Ei}^2} \right)$$

then

$$\begin{aligned} Y_1 &= A_1 * G_{11} + A_2 * G_{21} + A_3 * G_{31} \\ Y_2 &= A_1 * G_{12} + A_2 * G_{22} + A_3 * G_{32} \\ Y_3 &= A_1 * G_{13} + A_2 * G_{23} + A_3 * G_{33} \end{aligned}$$

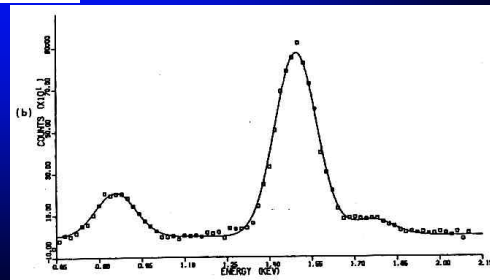
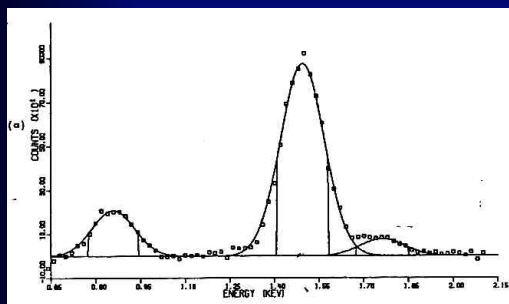
Using simple matrix algebra solve for A

•Fast and simple procedure

•Presumes operator knows all elements present

* System must be calibrated
(i.e. E_i and σ_{Ei} must be accurately known)

Spectral Processing : XEDS Curve Fitting : Linear Modeling



Spectral Processing : XEDS Curve Fitting : Non- Linear Modeling

Calculate and Minimize χ^2

$$\chi^2 = \sum_{k=1}^M \left(\sum_{i=1}^N \frac{(y_i - Y_k)^2}{y_i^2} \right) \quad \text{with } Y_k = A_k \exp \left(\frac{-(E_i - E_k)^2}{2\sigma^2(E_k)} \right)$$

and y_i = raw data

χ^2 is minimized by searching (E, A) parameter space

Pattern Search

- Sequential method: mechanical iteration of each parameter until a local minimum is found.
- Simplex method: simultaneous variation of all parameters.

Gradient Search

- Evaluate

Multiple Least Squares with Derivative Reference

- Linearization of the above problem
 $E \rightarrow E + \delta E$

$$I'(E) = I(E) - \delta E \frac{\delta I(E)}{\delta E} + \left(\sigma \delta \sigma + \frac{(\delta E)^2}{2} \right) \frac{\delta^2 I(E)}{\delta E^2}$$

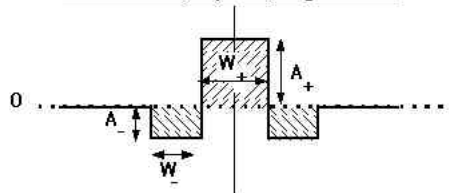
Spectral Processing : XEDS Digital Filtering

Background Suppression by Mathematical modeling

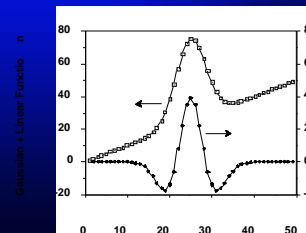
- Replace Data by new spectra formed by the following linear operation.

$$G(x_1) = [F(x_{+1}) - 2 * \left(\frac{W}{W_+} \right) * F(x_0) + F(x_{-1})] \quad \text{where } F(x_j) = \sum f(x_j)$$

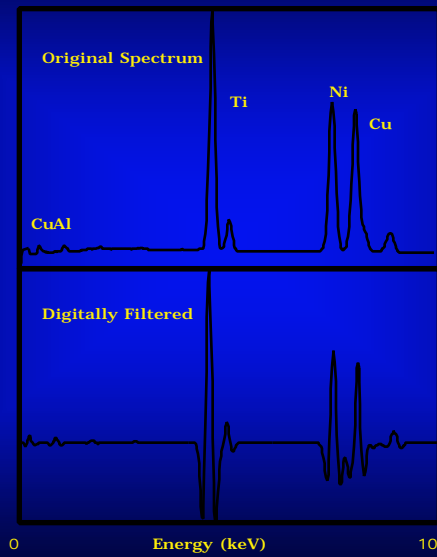
First Order (Top Hat) Digital Filter



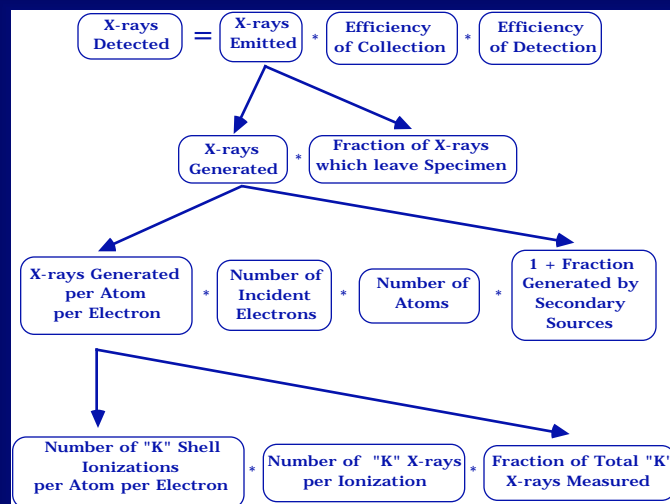
Operator independent
Introduces severe spectral distortion



Spectral Processing : XEDS Digital Filtering



X-ray Production



X-ray Production

$$I_A^K = \sigma_A^E \frac{\rho_A(E, Z)}{S_A} \left\{ R_A \right\} \left\{ f(\chi) \right\} \left\{ F_A \right\} C_A \frac{N_o}{W_A} \left\{ \rho_o A \right\}$$

I_A	=	Measured x-ray intensity per unit area
σ	=	K th -shell ionization cross-section
ω	=	K th -shell fluorescence yield
Γ	=	K th -shell radiative partition function
R	=	Backscatter Correction Term
S	=	Electron Stopping Power
$f(\chi)$	=	Absorption Correction Term
F	=	Fluorescence Correction Term
W	=	Atomic Weight
N_o	=	Avagadro's number
ρ	=	Density
C	=	Composition (At %)
ρ_o	=	Incident electron flux
t	=	Specimen thickness
ϵ	=	Detector efficiency
Ω	=	Detector solid angle

Quantification Procedures - Matrix Corrections

Empirical Models

Assume that each element linearly influences the x-ray intensity of each other element. Produce a table of coefficients to correct for inter-element effects

ZAF Corrections

Matrix effects are grouped into 3 categories and calculated
 Z - Atomic Number, A- Absorption, F - Fluorescence
 Deviations from Linearity (I vs C) are corrected by multiplicative terms

Phi-Rho-Z (ρ z)

Model the depth distribution of electron scattering and combine stopping power and absorption corrections

Monte Carlo

Individual electron trajectories simulated in a computer used mainly to simulate scattering and to formulate analytical equations for ZAF and (ρ z) methods or treat special geometries.

Quantitative Analysis using XEDS Standards Method

Invoke the Intensity Ratio Method, but now consider the ratio of the **same** x-ray line from two different specimens, where one is from a **standard** of known composition while the other is **unknown**:

$$\frac{I_U^K}{I_S^K} = \frac{\frac{I_U^K}{I_U^K} \cdot \frac{S_U(E,Z)}{S_U(E,Z)} \cdot \{R_U\} \cdot \{f(\lambda)\} \cdot \{F_U\} \cdot C_U \cdot \frac{N_o \cdot U}{W_U} \cdot \left\{ \frac{U}{o} \right\}}{\frac{I_S^K}{I_S^K} \cdot \frac{S_S(E,Z)}{S_S(E,Z)} \cdot \{R_S\} \cdot \{f(\lambda)\} \cdot \{F_S\} \cdot C_S \cdot \frac{N_o \cdot S}{W_S} \cdot \left\{ \frac{S}{o} \right\}}$$

$$\frac{I_U^K}{I_S^K} = \frac{\frac{I_U^K}{I_U^K} \cdot \frac{S_U(E,Z)}{S_U(E,Z)} \cdot \{R_U\} \cdot \{f(\lambda)\} \cdot \{F_U\} \cdot \left\{ \frac{U}{o} \right\} \cdot C_U}{\frac{I_S^K}{I_S^K} \cdot \frac{S_S(E,Z)}{S_S(E,Z)} \cdot \{R_S\} \cdot \{f(\lambda)\} \cdot \{F_S\} \cdot \left\{ \frac{S}{o} \right\} \cdot C_S}$$

$$\frac{I_U^K}{I_S^K} = \{K_Z\} \cdot \{K_A\} \cdot \{K_F\} \cdot \left\{ \frac{U}{S} \right\} \cdot \frac{C_U}{C_S}$$

These equations state that the **relative intensity ratio** of same characteristic x-ray line is directly proportional to the relative **composition ratio** of the two specimens multiplied by a some **correction terms** and **the beam current ratio**

Determining the k Factors

Experimental Measurements

Prepare standards of known composition
then measure relative intensities and solve explicitly
for the factor needed. Prepare a working data base.

This is the "best" method, but
- specimen composition must be verified independently
- must have a standard for every element to be studied

Theoretical Calculations

Attempt first principles calculation knowing
some fundamental parameters of the AEM system

Start with a limited number of k factor measurements,
then fit the AEM parameters to best match the data.
Extrapolate to systems where measurements and/or
standards do not exist.

Quantitative Analysis using XEDS Standardless Method

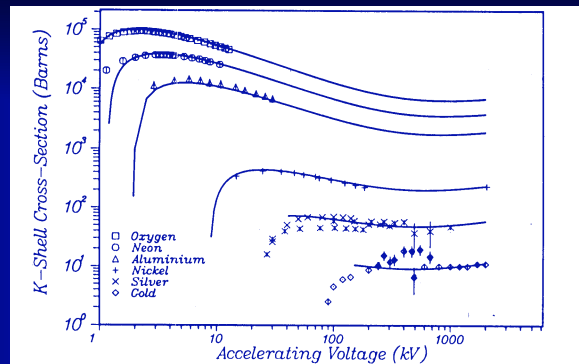
Invoke the Intensity Ratio Method, but now consider the ratio of the
different x-ray lines from the same specimen:

$$\frac{I_A^K}{I_B^K} = \frac{\frac{I_{A,A}^E}{S_A} \{R_A\} \{f(\)\} \{F_A\} C_A \frac{N_o}{W_A} \{ \rho_A \}}{\frac{I_{B,B}^E}{S_B} \{R_B\} \{f(\)\} \{F_B\} C_B \frac{N_o}{W_B} \{ \rho_B \}}$$

$$\frac{I_A^K}{I_B^K} = \frac{\frac{A}{E_c} \frac{A(E, Z)}{S_A} \{R_A\} \{f(\)\} \{F_A\} \frac{1}{W_A} \{ _A \} C_A}{\frac{B}{E_c} \frac{B(E, Z)}{S_B} \{R_B\} \{f(\)\} \{F_B\} \frac{1}{W_B} \{ _B \} C_B}$$

$$\frac{I_A^K}{I_B^K} = \{K_Z^{AB}\} \cdot \{K_A^{AB}\} \cdot \{K_F^{AB}\} \cdot \left\{ \frac{A}{B} \right\} \cdot \frac{C_A}{C_B}$$

Ionization Cross-Section



For K Shells

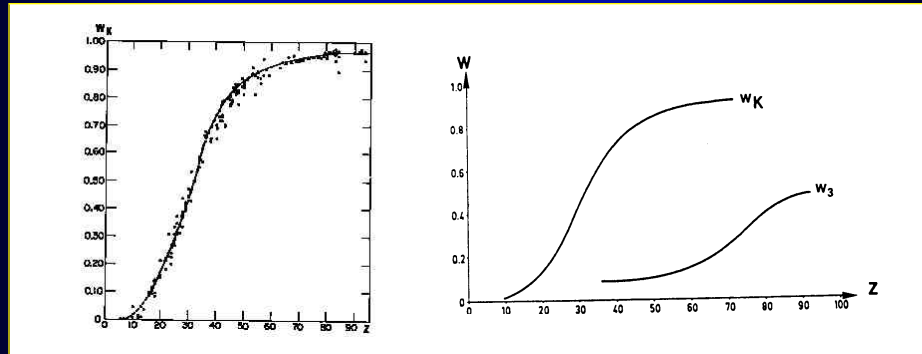
$$Q_K = \frac{a_K \cdot b_K \cdot \left\{ \ln \left(c_K \cdot \frac{T_0}{E_c} \right) - \ln(1-\beta^2) - \beta^2 \right\}}{T_0 \cdot E_c}$$

$T_0 = 1/2 m_0 c^2 \beta^2$, E_c = Shell Excitation Energy, $\beta = v/c$

For L Shells

$$Q_L = \frac{a_L \cdot b_L \cdot \left\{ \ln \left(c_L \cdot \frac{T_0}{E_c} \right) - \ln(1-\beta^2) - \beta^2 \right\}}{T_0 \cdot E_c}$$

X-ray Fluorescence Yield has Systematic Variation With Atomic Number



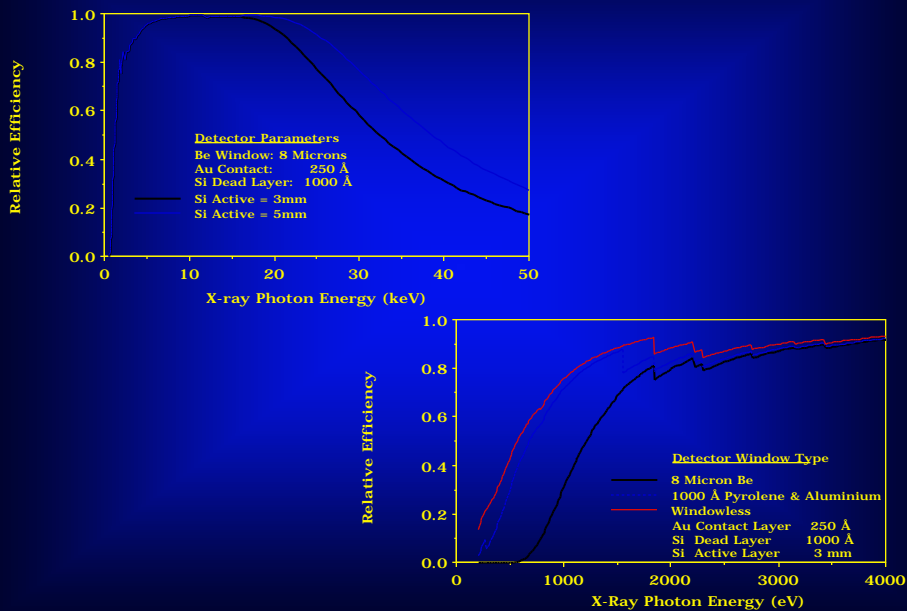
K shell

K vs L shell

Radiative Partition Function (Γ) Governs the Relative Intensities
Nominal Values (Varies slowly with Atomic Number)

K Shell	L Shell	M Shell
$K_{\alpha 1} = 100$	$L_{\alpha 1} = 100$	$M_{\alpha 1 2} = 100$
$K_{\alpha 2} = 50$	$L_{\alpha 2} = 50$	$M_{\beta} = 60$
$K_{\beta 1} = 15-30$	$L_{\beta 1} = 50$	
$K_{\beta 2} = 1-10$	$L_{\beta 2} = 20$	
$K_{\beta 3} = 6-15$	$L_{\beta 3} = 1-6$	
	$L_{\beta 4} = 3-5$	
	$L_{\gamma 1} = 1-10$	
	$L_{\gamma 2} = 0.5-2$	
	$L_{\eta} = 1$	
	$L_{\zeta} = 1-3$	

Calculated Si(Li) Detector Efficiency by Active Layer Thickness & Window Type

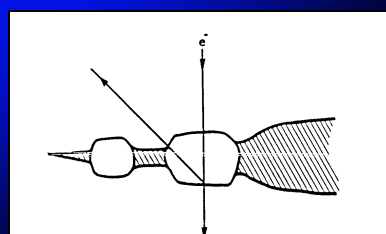
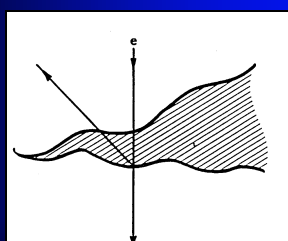
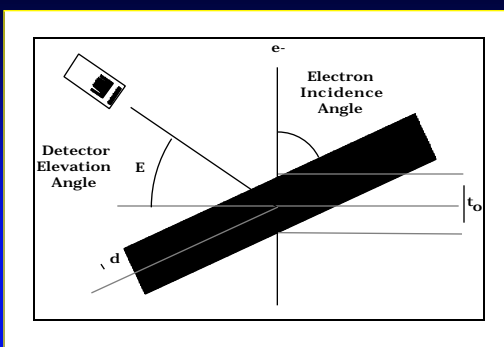


Sources of values for k_{AB} Calculations

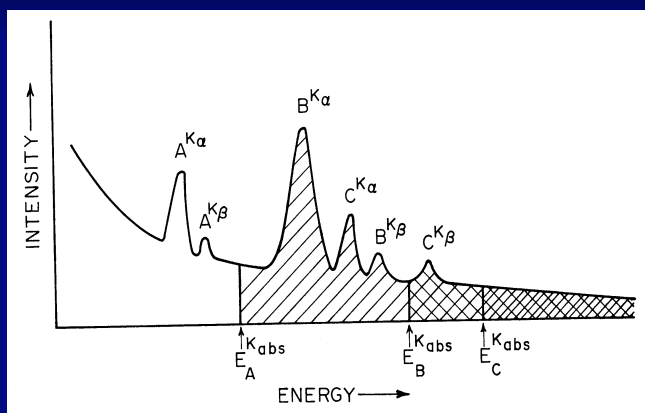
- W - International Tables of Atomic Weights
- (K) - Schreiber and Wims, X-ray Spectroscopy (1982)
Vol 11, p. 42
- (L) - Scofield, Atomic and Nuclear Data Tables (1974)
Vol 14, #2, p. 121
- (K) - Bambynek et al, Rev. Mod. Physics, Vol 44, p. 716
Freund, X-ray Spectrometry, (1975) Vol 4, p.90
- (L) - Krause, J. Phys. Chem. Ref. Data (1974) Vol 8,
p.307
- (Eo) - Inokuti, Rev. Mod. Physics, 43, No. 3, 297 (1971)
- Goldstein et al, SEM 1, 315, (1977)
- Chapman et al, X-ray Spectrometry, 12,153,(1983)
- Rez, X-ray Spectrometry, 13, 55, (1984)
- Egerton, Ultramicroscopy, 4, 169, (1969)
- Zaluzec, AEM-1984, San Fran. Press. 279, (1984)
- (E) - Use mass absorption coefficients from:
-Thinh and Leroux; X-ray Spect. (1979), 8, p. 963
-Henke and Ebsiu, Adv. in X-ray Analysis,17, (1974)
-Holton and Zaluzec, AEM-1984, San Fran Press,353,(1984)

X-Ray Absorption Correction

Path Length Out of the sample is the critical parameter



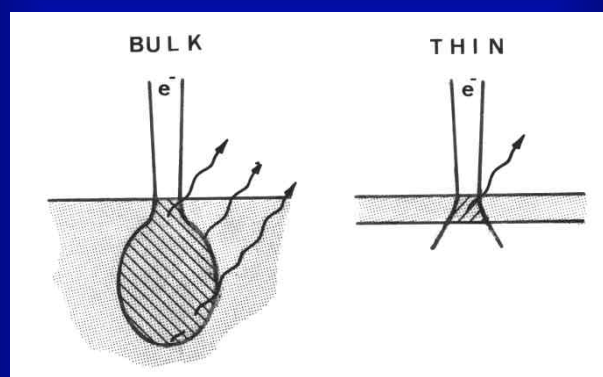
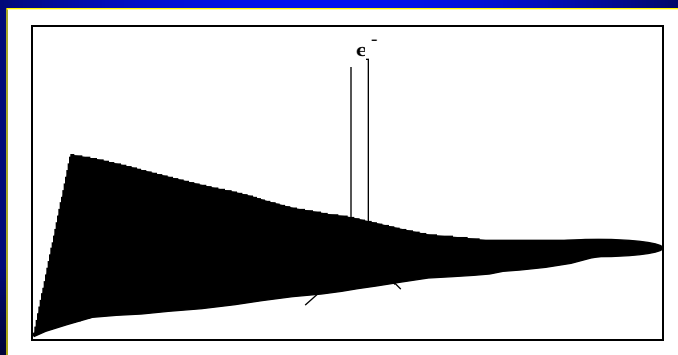
X-ray Fluorescence Correction Both Characteristic and Continuum X-rays



$$I_A^{\text{Measured}} = I_A^{\text{Electron}} + I_A^{\text{XRF by B}}$$

All quantitative analysis equations were derived assuming that the specimen is homogeneous over the excited volume

Application of these equations to heterogeneous specimens effectively averages the composition over the excited volume.



Quantitative Analysis using XEDS

For a thin specimen

$$I_A^{K\alpha} = \left\{ \sigma_A(E,Z) \Gamma_A \omega_A \right\} C_A \left\{ \frac{N_o \rho}{W_A} \right\} \left\{ \eta_o t \right\} \left\{ \epsilon_A \Omega \right\}$$

I_A	=	Measured x-ray intensity per unit area
	=	K^{th} -shell ionization cross-section
	=	K^{th} -shell fluorescence yield
	=	K^{th} -shell radiative partition function
W	=	Atomic Weight
N_o	=	Avagadro's number
	=	Density
C	=	Composition (At %)
ϵ_o	=	Incident electron flux
t	=	Specimen thickness
	=	Detector efficiency
	=	Detector solid angle

Quantitative Analysis using XEDS Standardless Method

Invoke the Intensity Ratio Method, that is consider the ratio of x-ray lines from two

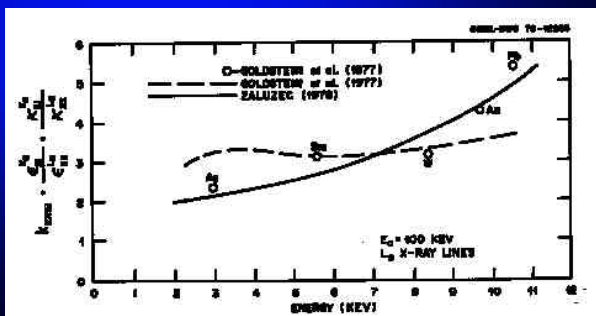
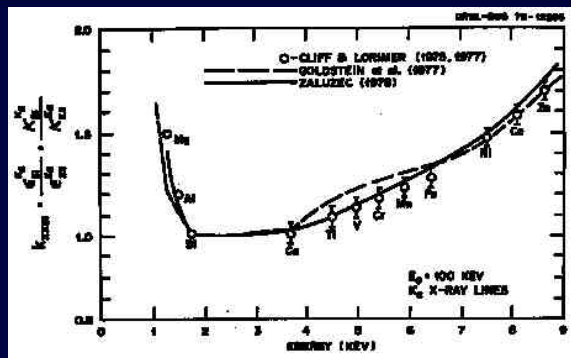
$$\frac{I_A}{I_B} = \frac{\kappa_A \epsilon_A C_A}{\kappa_B \epsilon_B C_B} = k_{AB}^{-1} \frac{C_A}{C_B}$$

$$\kappa_A = \frac{\sigma_A \omega_A \Gamma_A}{W_A}$$

$$\frac{\kappa_A \epsilon_A}{\kappa_B \epsilon_B} = k_{AB}^{-1} \quad (\text{k-factor})$$

This simple equation states that the relative intensity ratio of any two characteristic x-ray lines is directly proportional to the relative composition ratio of their elemental components multiplied by some "constants" and is independent of thickness.

NOTE: The k_{AB} factor is not a universal constant!!
Only the ratio of k_A/k_B is a true physical constant and is independent of the AEM system. The ratio of ϵ_A/ϵ_B is not a constant since no two detectors are identical over their entire operational range. This can cause problems in some cases as we shall see.



Quantitative Analysis using XEDS Thin Film Standards Method

Invoke the Intensity Ratio Method, but now consider the ratio of the same x-ray line from two different specimens, where one is from a **standard** of known composition while the other is **unknown**:

$$\frac{I_u}{I_s} = \frac{\eta_u \rho_u t_u}{\eta_s \rho_s t_s} \cdot \frac{C_u}{C_s}$$

$$C_u = \frac{\eta_s \rho_s t_s}{\eta_u \rho_u t_u} \cdot \frac{I_u}{I_s} \cdot C_s$$

This simple equation states that the relative intensity ratio of same characteristic x-ray line is directly proportional to the relative composition ratio of the two specimens multiplied by a some new parameters.

η = incident beam current
 ρ = local specimen density
 t = local specimen thickness

Advantages

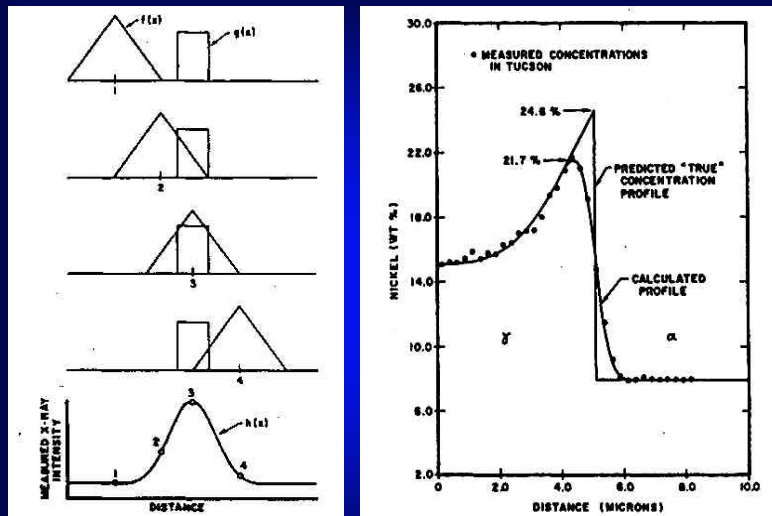
Standard may be a pure element.
The closer the standard is to the
unknown material the smaller the
correction and higher the accuracy.

Disadvantages

Effects of surface films can be critical
Must have a standard for each element
to be analyzed

Additional Topics

Heterogeneous Specimens
Composition Profiles
Mapping
ESEM
Electron Channelling



$$C^*(x,y) = C(x,y,z) * d(x,y,z)$$

$C^*(x,y)$ = Apparent profile measured

$C(x,y,z)$ = Actual composition profile

$d(x,y,z)$ = Incident beam profile

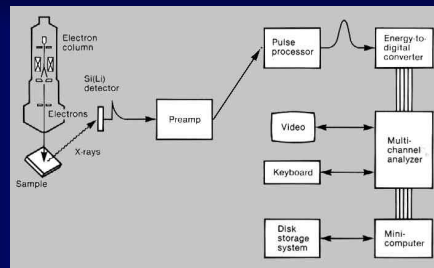
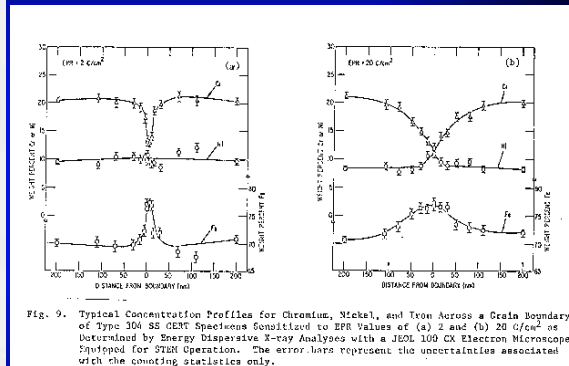
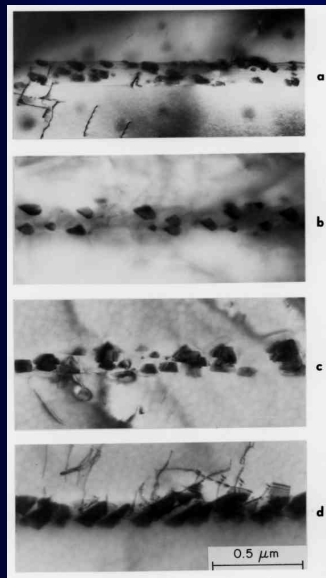
$*$ = Convolution operator

F, F^{-1} = Fourier and Inverse Fourier Transforms

In the 2 dimensional limit one can deconvolute the measured profile using:

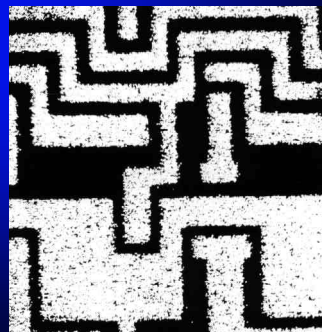
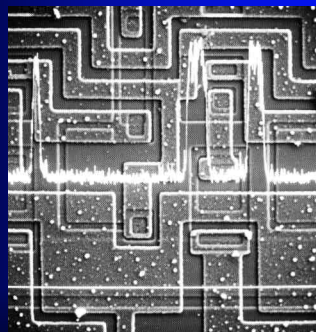
$$C(x,y) = F^{-1} \left[\frac{F[C^*(x,y)]}{F[d(x,y)]} \right]$$

Realistically, it is better to decrease the probe diameter and specimen thickness

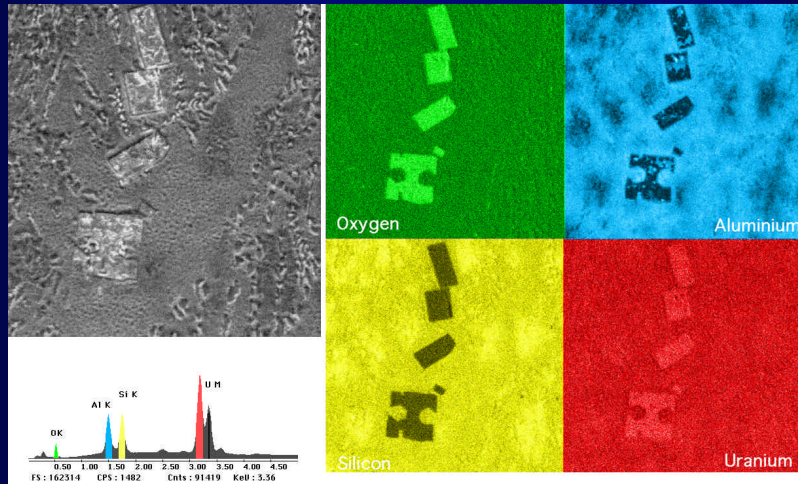


Analog "Dot" Maps

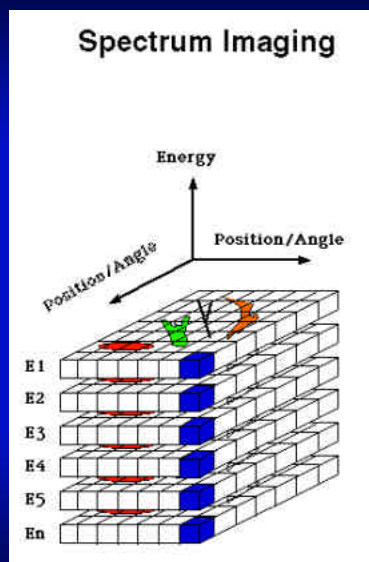
Good for Major Species
Overlaps can prohibit mapping
Low Conc. very difficult

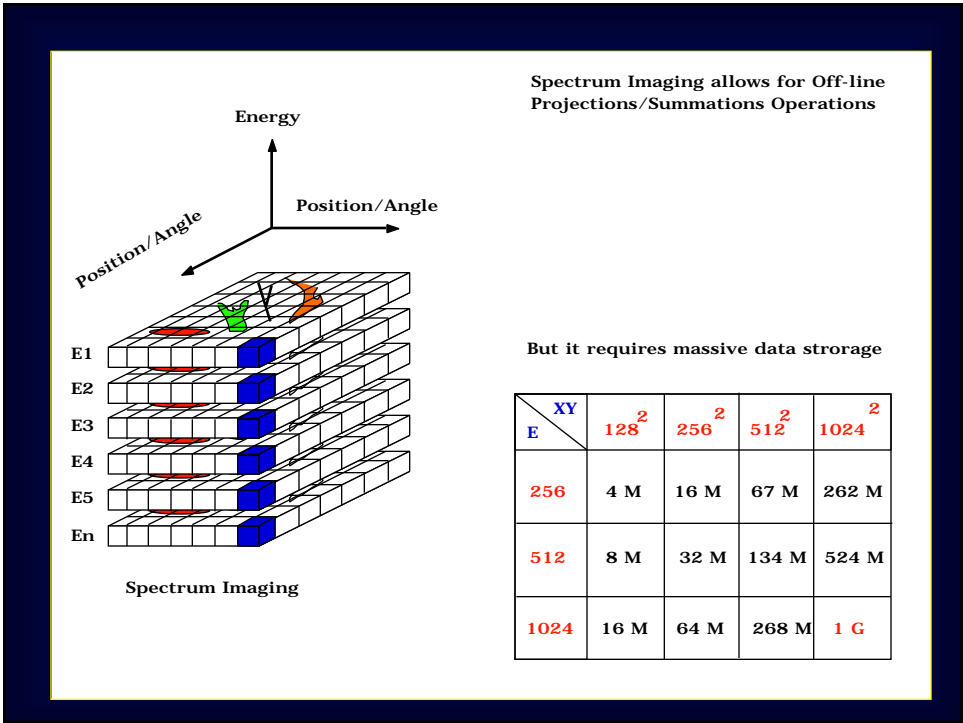
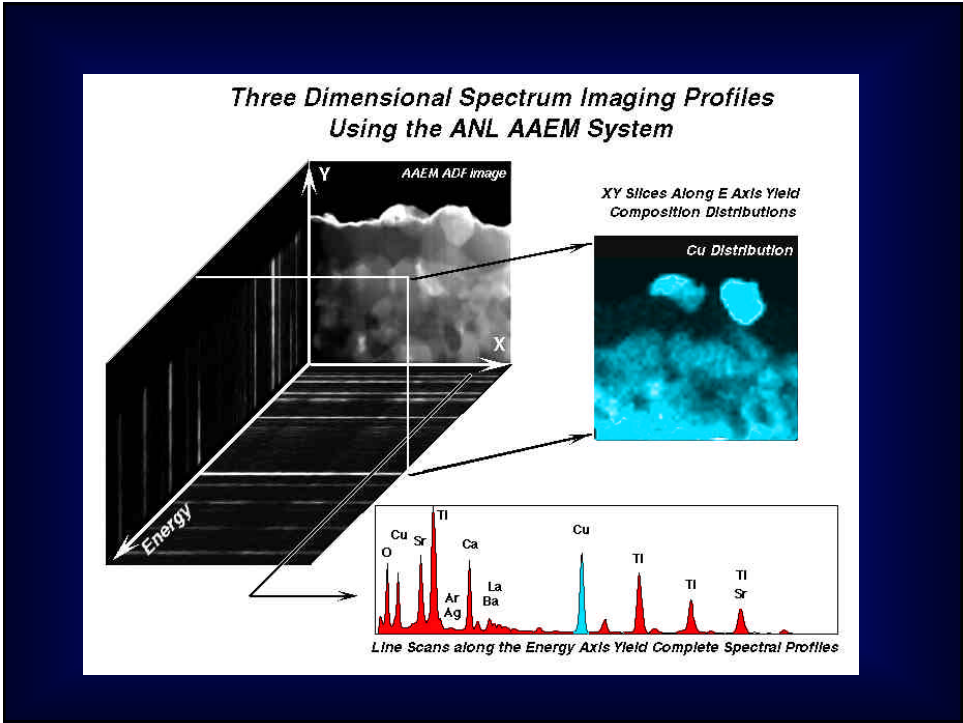


Digital Mapping

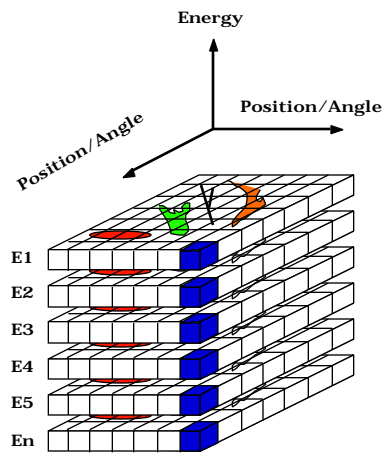
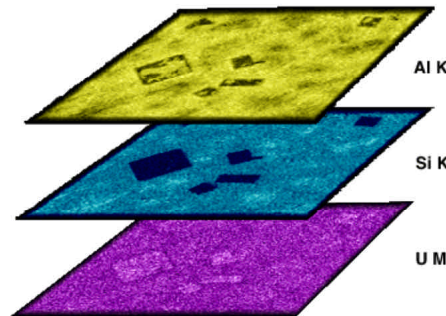
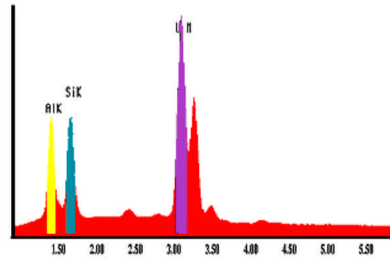
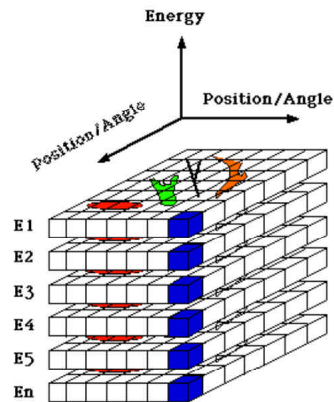


Computationally Mediated - Spectral Imaging





Spectrum Imaging



Spectrum Imaging

XY t	128 ²	256 ²	512 ²	1024 ²
1 μ s	16 ms	65 ms	0.26 s	1.05 s
1 ms	16 s	65 s	4.4 min	17.5 min
1 s	~4.5 hrs	~18 hrs	~3 days	~12 days
1 min	~11 days	~1.5 mnths	~6 mnths	~2 yrs

**X-RAY MICROANALYSIS IN
ENVIRONMENTAL / VARIABLE PRESSURE
SEM**

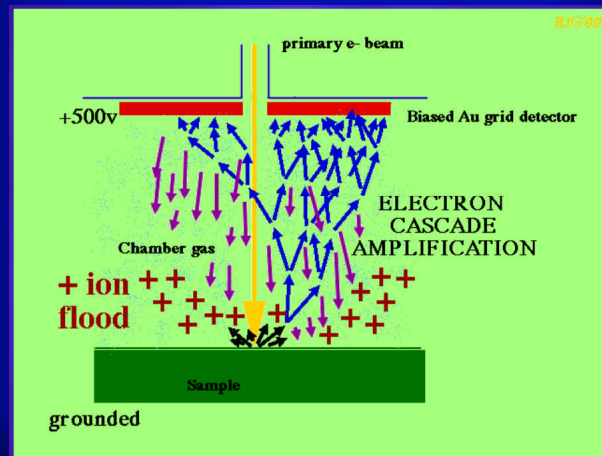
Courtesy of B.J. Griffin

VPSEM/ESEM allow examination of a wide range of untreated samples because:

- **Conventional wisdom suggests that charge neutralisation for poor and non-conductive materials through gas-electron interaction is effective**

*Early work states that this neutralisation occurs with Ar
chamber pressures of only 0.1 torr - BSEI stability
(Nickel and Robinson, 1979)*

Conventional/current 'SE' detection in conventional and variable pressure (VP) SEM



KNOWN COMPROMISES

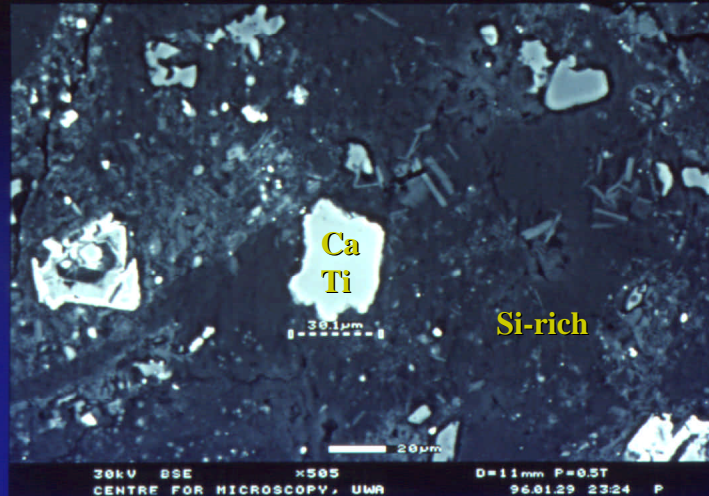
- Gas-electron interactions radially scatter the primary electrons away from the intended landing point = $f(\text{gas, pressure, path length \& } E_0)$
- Primary beam current cannot be directly measured and it fluctuates with pressure

X-ray maps are diffuse & point analyses need normalisation

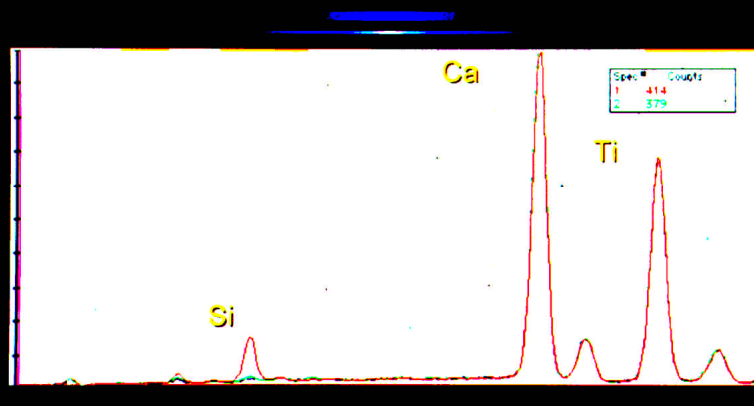
Gas scatter effects on EDS spectra

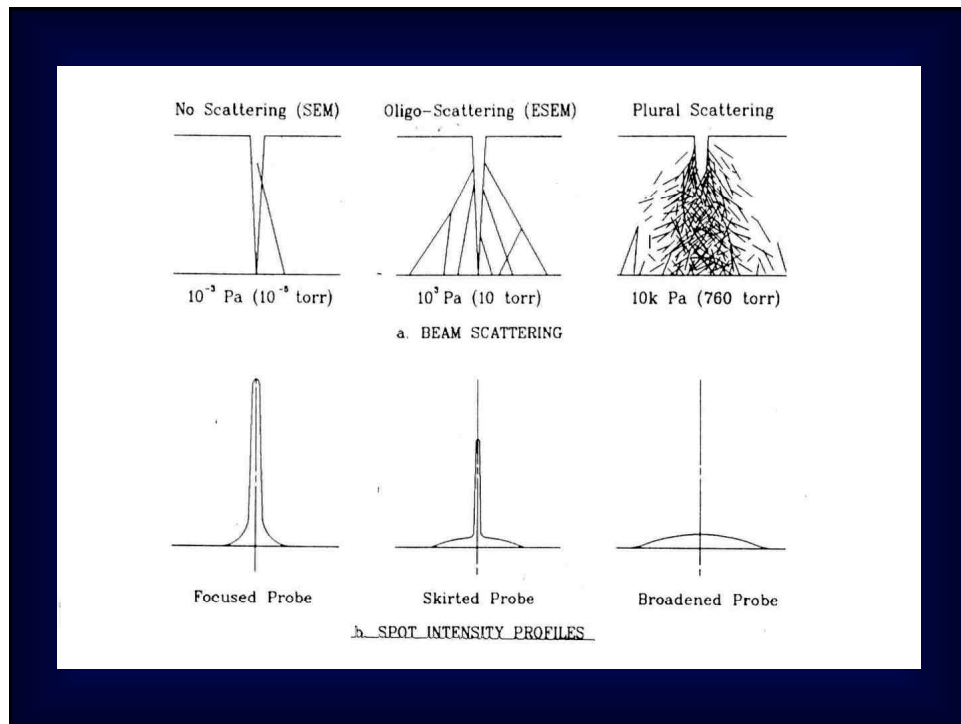


ESEM BSEI of Perovskite grain



ESEM - Perovskite spectra



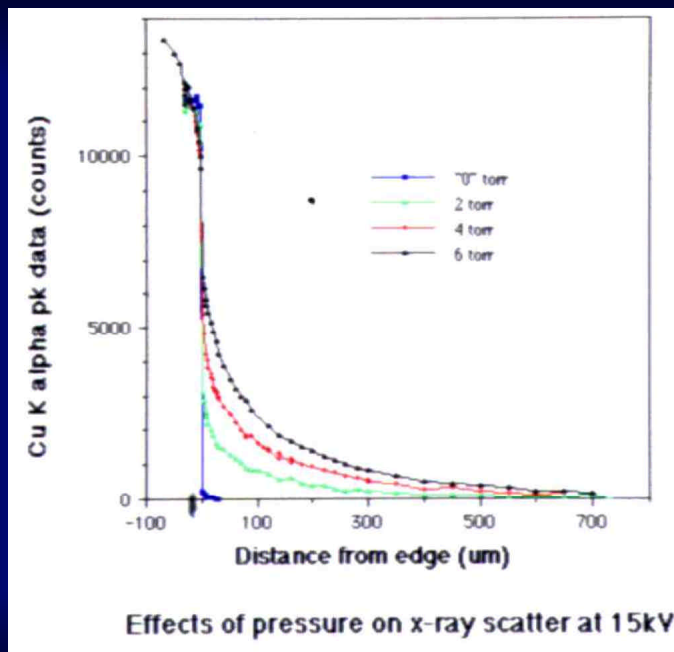
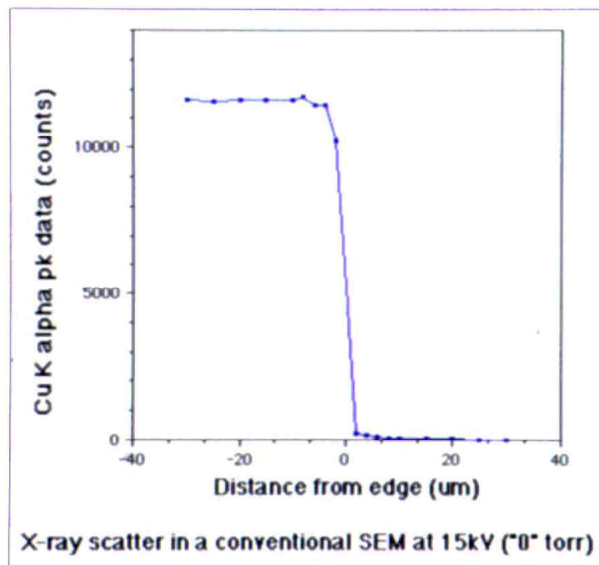


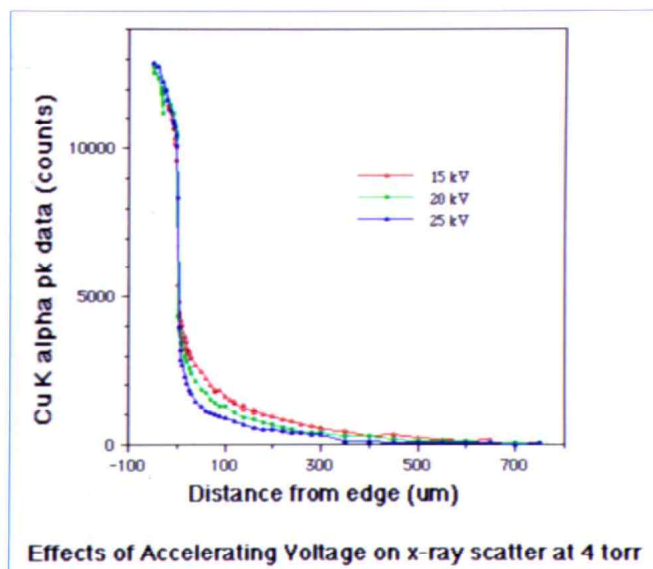
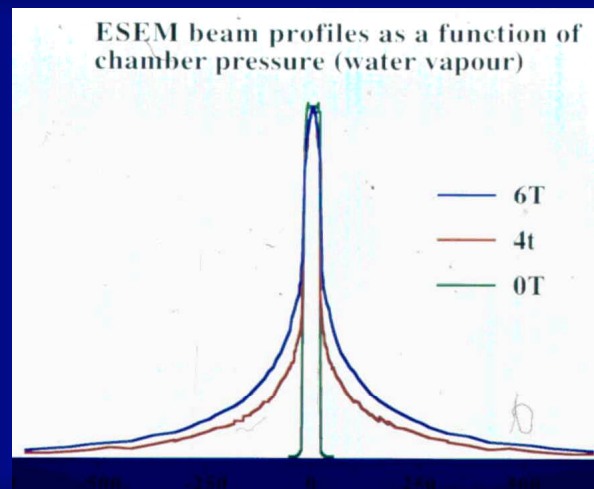
PLA extension to minimise scatter

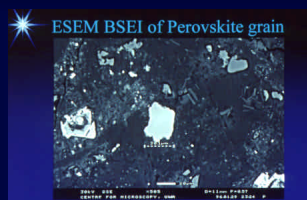
Intermediate region

Specimen chamber

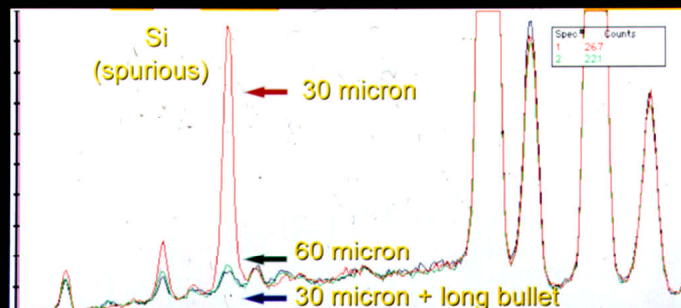
- Reduce the gas pressure.
- Work in He environment.
- Reduce the path length within the gas.







Gas scatter effects on EDS spectra

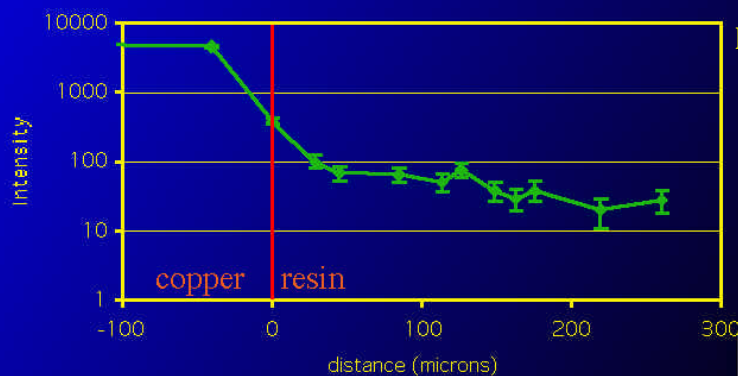


Kimberlite rock sample: 30 kV, 0.5 torr, 10mm WD

Gas scatter effects on EDS spectra

Spatial resolution test

Cu L intensity v's distance



He gas,
0.1 torr,
3 kV,
long PLA

- Intensity of Cu L line is 1.7% of the pure Cu L_{α} intensity 30 microns away from Cu-resin interface.

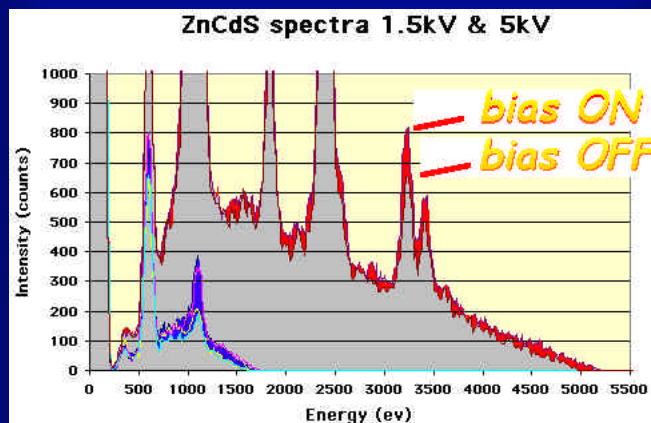


Other factors compromising EDS quantitation

POTENTIAL EFFECTS ON THE ACCELERATING VOLTAGE due to:

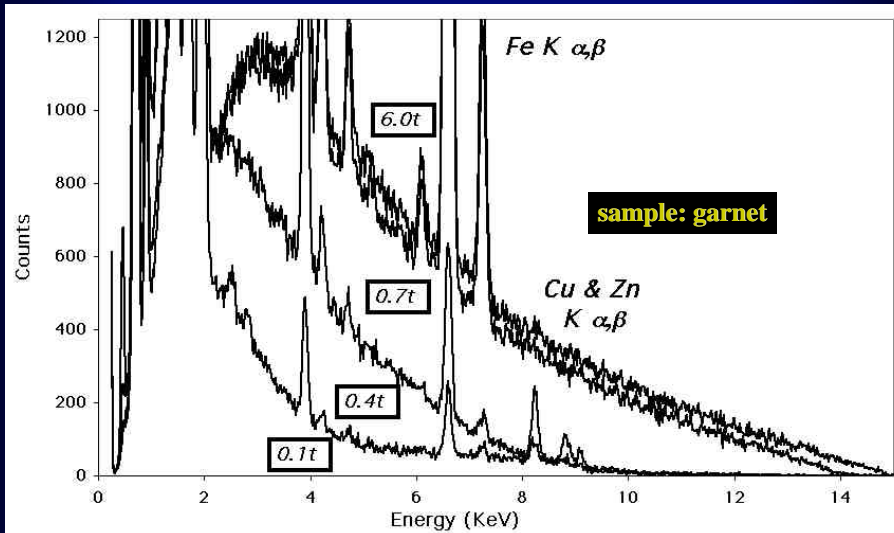
- increase in landing energy of the primary beam
ie secondary acceleration
- by positive surface or 'space' charge
- decrease in landing energy of the primary beam as a result of incomplete charge neutralisation or charge implantation in the sample

Positive 'space' charge



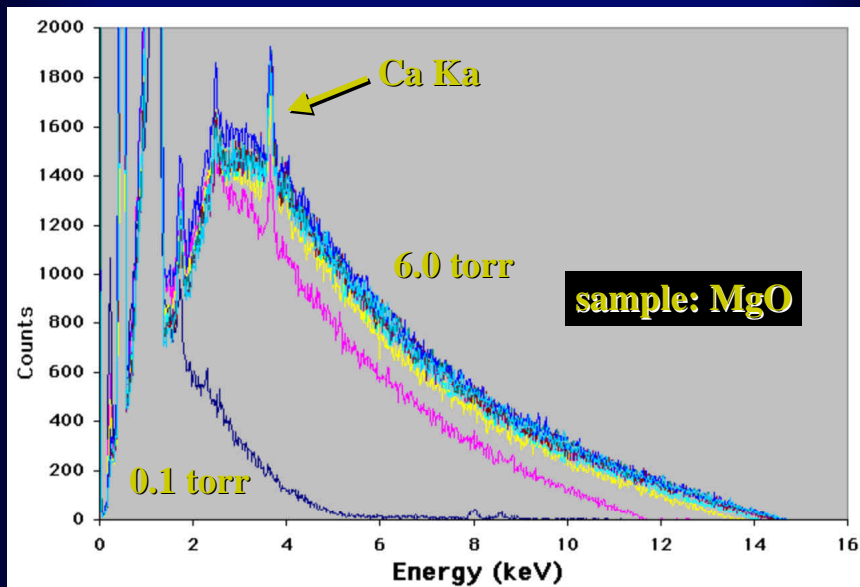
Effects on low kV EDS spectra of increases in electron landing energy as a function of ESD bias
- "floating" conductive sample

Charging/Pressure effects on EDS spectra



Spectra collected at 15 kV, 11mm gpl, H₂O, 100 sec & "3000" cps

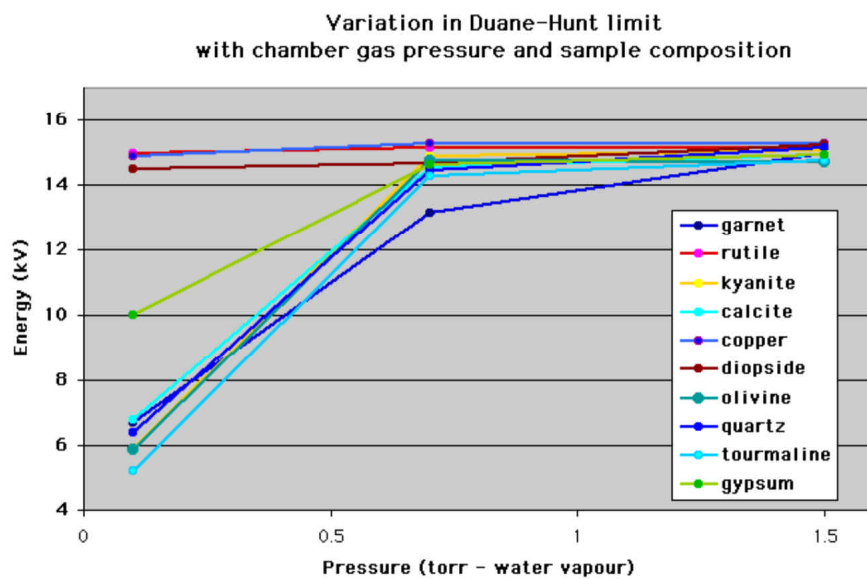
Charging/Pressure effects on EDS spectra



Effects of varying pressure on EDS spectra

- EDS spectra vary with chamber pressure
- Duane-Hunt limit changes and indicates a negative charging of the sample
- sample charging effects are present even at moderate chamber pressures
- electrostatic mirror formation at low pressure - results in addition of high E x-rays from chamber components imposed on low "E₀" sample spectrum

D-H limit variat'n with composition



Summary - charging effects

These data support earlier work and confirm that:

- poorly conductive samples charge **NEGATIVELY** in VPSEM/ESEM under most routine conditions
- reducing the gas path length does not avoid the problem
- the gaseous secondary electron detector bias is a factor in the degree of charging experienced
- sample composition is a major factor in the degree of charging experienced
- this is extendable to sample size and analysis point location

Implications for quant. microanalysis

- beam dose must be kept constant and monitored - to avoid temporal effects
- standards **MUST** have similar conductive properties to the unknowns
- otherwise electron landing energies will differ and incorrect matrix corrections applied
- the Duane-Hunt limit should always be monitored
- moderate to high pressures should be used and extended PLA to minimise scattering effects
- the Bremsstrahlung-based correction procedure may need reconsideration

Conclusions - EDS in VPSEM/ESEM

- a wide range of factors can significantly affect EDS x-ray spectra collected in VPSEM/ESEM
- charging effects are seen up to ~ 2.0 torr and extreme caution must be used in collection and interpretation of this type of data
- charging effects vary with sample composition
- applications exist where the VPSEM/ESEM have unique microanalytical strengths
- quantitative microanalysis at conventional / acceptable levels remains difficult at present

**<http://tpm.amc.anl.gov/Lectures/XEDS-Apr2001.pdf>
(not until Monday)**

**Zaluzec@aaem.amc.anl.gov
Zaluzec@microscopy.com**